Chemical Science

ROYAL SOCIETY OF CHEMISTRY

PERSPECTIVE

View Article Online
View Journal | View Issue

Cite this: *Chem. Sci.*, 2024, **15**, 17760

All publication charges for this article have been paid for by the Royal Society of Chemistry

Received 11th July 2024
Accepted 15th October 2024

DOI: 10.1039/d4sc04608k

rsc.li/chemical-science

Two in one: merging photoactivated chemotherapy and photodynamic therapy to fight cancer

Kirill M. Kuznetsov, Kevin Cariou * and Gilles Gasser *

The growing number of cancer cases requires the development of new approaches for treatment. A therapy that has attracted the special attention of scientists is photodynamic therapy (PDT) due to its spatial and temporal resolution. However, it is accepted that this treatment methodology has limited application in cases of low cellular oxygenation, which is typical of cancerous tissues. Therefore, a strategy to overcome this drawback has been to combine this therapy with photoactivated chemotherapy (PACT), which works independently of the presence of oxygen. In this perspective, we examine compounds that act as both PDT and PACT agents and summarize their photophysical and biological characteristics.

1. Introduction to PDT and PACT

The World Health Organization (WHO) expects that the number of new cases of all types of cancer will grow from 20 million in 2022 to 33 million in 2045.[1] The increasing number of cancer cases raises a significant concern, urging us to closely examine contributing factors and develop innovative approaches for better understanding, detection, and treatment of this disease. One example of such an innovative therapeutic approach is the clinically approved method called photodynamic therapy (PDT). PDT is based on the interactions of a photosensitizer (PS) with light in the presence of oxygen.

To better understand the processes, let us turn to the Jablonski diagram depicted in Fig. 1. Under irradiation, the PS absorbs light, and an electron of the ground state transfers to a higher-lying electronic singlet state.[2,3] The molecule then relaxes to the lowest vibrational state without emitting a photon. In addition to the radiative transition to the ground state (fluorescence), a non-radiative relaxation to the triplet state can occur. This process is called intersystem crossing (ISC) and has a higher probability of happening in the presence of a heavy atom. In both singlet and triplet excited states, a reaction with oxygen is possible. The triplet state of oxygen ($^3O_2$) shows generally much higher reactivity rates, leading to the formation of singlet oxygen ($^1O_2$) from $^3O_2$ by energy transfer.[4] This $^1O_2$ is highly reactive and can interact with surrounding

Chimie ParisTech, PSL University, CNRS, Institute of Chemistry for Life and Health Sciences, Laboratory for Inorganic Chemical Biology, 75005 Paris, France. E-mail: gilles.gasser@chimieparistech.psl.eu; kevin.cariou@chimieparistech.psl.eu; Web: http://www.gassergroup.com/; Tel: +33 1 85 78 41 51

Kirill M. Kuznetsov

Kirill Kuznetsov completed his Master's degree at St. Petersburg State University (Saint Petersburg, Russia) in 2022. His early research focused on iridium, ruthenium, and europium complexes for bioimaging purposes. Since 2022, under the supervision of Gilles Gasser and Kevin Cariou at Chimie ParisTech, he has been working on his PhD thesis, developing new agents for photodynamic therapy and photoactivatable chemotherapy.

Kevin Cariou

Kevin Cariou received his PhD in 2006 from Sorbonne Université under the supervision of Max Malacria and Louis Fensterbank. From 2007 to 2009, he worked as a postdoctoral researcher in the group of Alison Frontier at the University of Rochester (NY, USA). He was appointed as a CNRS Researcher in 2009 at the Institut de Chimie des Substances Naturelles in the team led by Robert Dodd. He obtained his HDR in 2015 and moved to Chimie ParisTech in 2020 and was appointed Director of Research in 2021. His interests lie in the development of synthetic methods to access biologically active molecules.

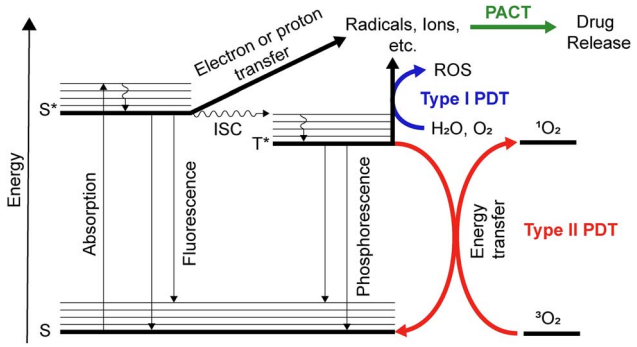

Fig. 1 Jablonski diagram depicting common pathways. Straight lines indicate radiative transitions. Curved arrows indicate non-radiative transitions. Bold arrows indicate processes of electron, energy, or proton transfer. S – singlet state, T – triplet state, * – excited state, ISC – intersystem crossing, PDT – photodynamic therapy, PACT – photoactivated chemotherapy, and ROS – reactive oxygen species.

molecules.[5] In particular, in biological systems, this generation of $^1O_2$ can be used to kill cancer cells. In the context of PDT, the $^1O_2$ generation process is referred to as Type II PDT. Type I PDT refers to an electron transfer between the excited PS and the surrounding molecules. Such interaction can lead to the formation of other types of reactive oxygen species ($OH^{\bullet}$, H_2O_2, $O_2^{-\bullet}$, *etc.*).[3] Both strategies can be utilized for cancer therapy, by using light as a trigger for the generation of toxic species, allowing spatial and temporal control of the therapy.[6–8] Electron transfer is also possible from triplet and singlet excited states to form radical molecules, ions, and other species, which are then converted to degradation products. This type of phototransformation is used in photoactivated chemotherapy (PACT).

The term PACT was proposed by Sadler in 2009.[8] PACT is similar to Type I PDT and occurs due to electron transfer of the triplet excited state of the compound (Fig. 1). As a result, degradation of the compound with radical formation or the formation of aqua species is possible.[9,10] The latter is most typical for ruthenium complexes.[11–15] The resulting compounds of degradation and their derivatives may exhibit toxicity against cancer cells. If so, it can be used for anticancer therapy. PACT usually does not require the presence of triplet oxygen; thus, it can be considered oxygen-independent compared to PDT.[16] However, compared to PDT, PACT is stoichiometric due to the irreversibility of transformation reactions, while PDT is catalytic due to the reversibility of excitation and relaxation processes to the ground state.

Being active even in hypoxia is especially important when the disease targeted is cancer as a common feature of the tumor microenvironment is hypoxia.[17] Several PDT agents are approved worldwide for clinical use, others underwent or are undergoing clinical trials.[18] PDT is usually characterized by low side effects and less likelihood of drug resistance.[19] Recently, more sophisticated strategies have been proposed combining PDT and sonodynamic therapy,[20] photothermal therapy,[21,22] hyperthermia,[23] radiotherapy,[24] chemotherapy,[25] and others.[26,27] One of the recent trends is to try to combine PDT with PACT.[6]

In this perspective, we summarize the known examples of dual PDT/PACT agents. We considered only single molecules that exhibited the properties of a PS before and/or after drug release and for which the released drug was found to be cytotoxic. Quite similar to photocages,[28] PDT/PACT agents can be divided into types depending on the nature of the PS: metal complexes and organic compounds.

2. Metal complexes as photosensitisers

Metal complexes are a rapidly growing class of PDT/PACT dual agents. Among the factors that are described in the literature rationalizing the choice of metal complexes are their thermal stability, as well as the stability of the excited state they can reach.[29,30] In the case of excited state stability, the ligand field should be discussed. Ligands exert a much weaker ligand field on 3d metals than on 4d- or 5d metals, since the more compressed 3d orbitals have weaker spatial overlap. This means that complexes with less overlap have a higher probability of transitioning to the ground state without light irradiation.[31] The latter limits the use of these metal complexes as PSs. One of the most informative reviews in the field of ruthenium complexes for PACT purposes was authored by Bonnet in 2023.[29] In our perspective, when describing ruthenium complexes and other compounds acting as dual agents, we highlight the absorption range, the quantum yields of singlet oxygen, the mechanism of release, the cytotoxicity of compounds, and the types of cells that were used to evaluate the anticancer effect of the compounds.

2.1. Ruthenium complexes

There are currently a growing number of ruthenium(II) complexes acting as PDT/PACT agents.[32] We can identify three factors influencing their ability to release ligands that would act as cytotoxic drugs: (1) the releasing ligand is mostly

Gilles Gasser

Gilles Gasser started his independent scientific career at the University of Zurich (Switzerland) in 2010 before moving to Chimie ParisTech, PSL University, in 2016 to take a PSL Chair of Excellence. Gilles was the recipient of several fellowships and awards including the Alfred Werner Award from the Swiss Chemical Society, an ERC Consolidator Grant and Proof of Concept, the European Bio-Inorganic Chemistry (EuroBIC), the Pierre Fabre Award for therapeutic innovation from the French Société de Chimie Thérapeutique and recently the Coordination Chemistry Prize from the French Chemical Society (Senior Level). Gilles' research interests lie in the use of metal complexes in different areas of medicinal and biological chemistry.

monodentate pyridine derivatives,[11,16,33–35] (2) other ligands are bipyridine or terpyridine derivatives,[16,33–36] and (3) they have substituents close to coordinated nitrogen.[16,34,35] The nature of the excited state of the metal complexes can explain the first and second factors. The coordination of bipyridine and terpyridine ligands leads to a stable ^{3}MLCT excited state of the complexes, which is reflected in high levels of singlet oxygen generation and relative photostability.[10] It can also be noted that the ruthenium complexes obtained for PACT purposes with S-coordinated ligands exhibited in most cases extremely low quantum yields of singlet oxygen or the yields were not measured.[12,13,37–39] The third factor appears to be related to steric hindrance, which helps to release a target ligand more easily.[29,40] Similarly, the elongation of the aromatic ligand system leads to mixed photoreactivity, combining both PACT and PDT mechanisms.[15] Interestingly, these complexes may not follow the energy gap law, which means that the complexes with the lowest energy ^{3}MLCT excited states are less able to efficiently populate the dissociative state.[41] A more detailed explanation of the interconnections between the structure and release rates can be found in the 2015 publication by Turro *et al.*[42] and related articles with computational studies.[9,43–47]

In 2017, Bonnet *et al.* reported red-light-activated ruthenium-caged nicotinamide phosphoribosyltransferase (NAMPT) inhibitors **1** and **2** (Fig. 2).[16] NAMPT is a key enzyme in NAD^+ biosynthesis and usually has elevated levels in cancer cells. The inhibitors selectively block NAMPT-dependent pathways and have the potential to be used as a tool in biomedical research. The quantum yields of singlet oxygen are <0.5% and 3.6% in CD_3OD, and the quantum yields of photodissociation are 5.8% and 1.3% in water solution, respectively. In general, it is believed that compounds with quantum yields of photodissociation in the 1–10% range are considered to be the most efficient.[29] Both compounds can be excited using blue and green light (λ_{abs} = 473 and 531 nm, respectively). Changing the nature of the ligand led to a major change in the photophysical properties. Four cell lines were used for cytotoxicity studies: three human cancer cell lines A549 (human lung adenocarcinoma), MCF-7 (human breast adenocarcinoma), and A431 (human epidermoid carcinoma), and a non-cancerous cell line MRC-5 (human lung). Half maximal effective concentrations (EC_{50}) were calculated under hypoxic (1% O_2) and normoxic conditions (21% O_2). It was found that the cytotoxicity of complex **2** is substantial in all cancerous cell lines in comparison with compound **1**. While compound **1** had no difference in hypoxia and normoxia, compound **2** was even more effective in hypoxia. The authors showed that the inhibitor activity released from complex **2** was comparable to the drug itself. The same complex has half-maximal inhibitory concentration IC_{50} = 4.8 μM before irradiation and IC_{50} = 0.26 μM after irradiation in comparison with a free drug with IC_{50} = 0.25 μM. Thus, it was demonstrated for the first time the use of dual agents as NAMPT inhibitors.

One of the first studies devoted to ruthenium(II) complexes as PDT/PACT agents was performed in Turro's lab in 2015.[40] Initially, the obtained compounds were not characterized using biological assays. Fortunately, the group continued to work in this area,[15] and in 2018, they published a paper discussing complexes **3–5**, which are derivatives of the chemotherapeutic drug imatinib (Fig. 3).[48] Imatinib, known as a tyrosine kinase inhibitor, is commonly prescribed for treating gastrointestinal stromal tumors. The study explored the potential of photocontrollable drug release to mitigate side effects associated with imatinib, such as abdominal pain, decreased hemoglobin, nausea, vomiting, cardiac toxicity, and skin issues. The metal complexes exhibited a high quantum yield of singlet oxygen (7.3–25%) with an absorption spectrum extending up to 650 nm. Compound **5** also showed a significant 57% quantum yield

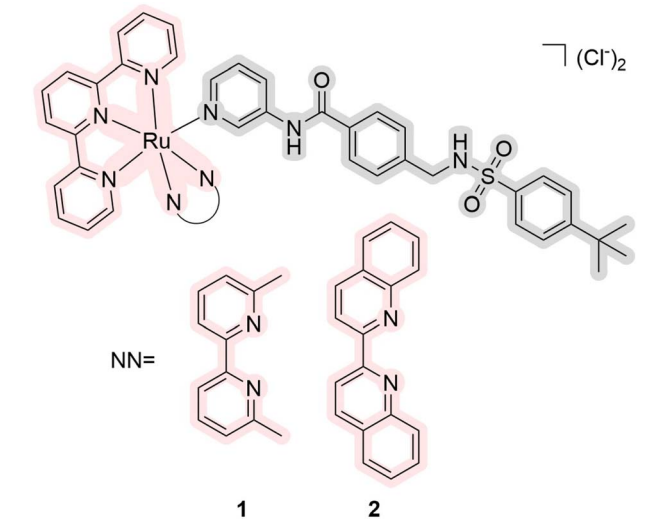

Fig. 2 Structures of ruthenium complexes **1** and **2** as prodrugs of enzyme inhibitors that exhibit properties of PDT/PACT agents. Light pink highlights a part of PS, while gray indicates the released ligand.

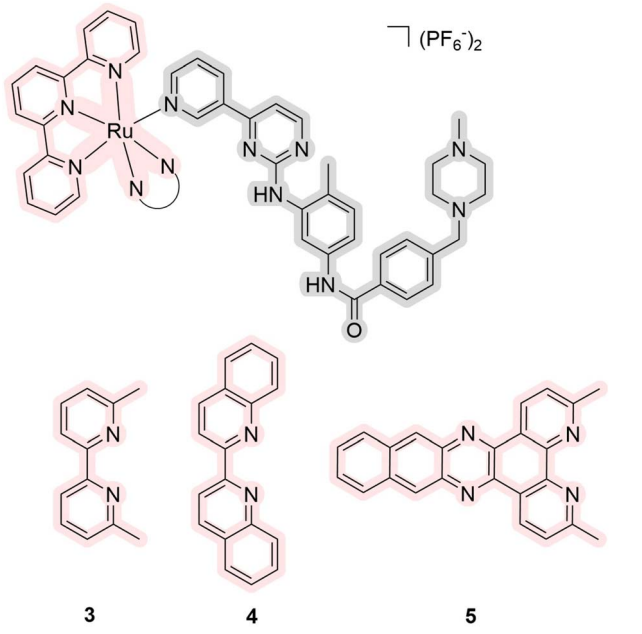

Fig. 3 Structures of ruthenium complexes **3–5** as prodrugs of enzyme inhibitors that exhibit properties of PDT/PACT agents. Light pink highlights a part of PS, while gray indicates the released ligand.

of drug photorelease under 500 nm irradiation. Although there are no *in vivo* assays for the compound, the study examined its affinity for the gene encoding the receptor tyrosine kinase protein (C-kit/CD117). For this purpose, derivatives of these metal complexes were prepared with a carboxyl group that readily binds to an antibody targeting the receptor tyrosine kinase protein. The studies showed that conjugation with the antibody did not affect the release of imatinib. Thus, the authors obtained a dual PDT/PACT agent targeting the receptor tyrosine kinase protein capable of releasing a chemotherapeutic drug.

In 2021, Zhou's group reported ruthenium(II) complexes **6** and **7** that were expected to have three functions: PDT agents, PACT agents, due to the bipyridine-containing quinone fragment, and catalysts of photooxidative processes (Fig. 4).[36] Quinones are known to be actively involved in mitochondrial respiration. With this in mind, the authors have proposed a nitro-anthraquinone moiety that can accept an electron from the excited ruthenium moiety, oxidizing the metal centre and releasing the ligand with this anthraquinone-based anionic moiety. The latter can serve as a photooxidative catalyst, causing cellular oxidative stress. The absorption spectrum of the compounds had an absorption maximum at 560 nm with a tail of the spectrum up to 700 nm. The authors did not provide the values of quantum yields of photorelease, but when the compounds were photo-irradiated at 600 nm for 25 min in acetonitrile, the authors observed photodissociation with yields of 72% and 47%, respectively. In studies with 9,10-anthracenediyl-bis(methylene)dimalonic acid, the compounds did not show the ability to generate singlet oxygen but showed the possibility of generating $O_2^{-\bullet}$ with dihydroethidium. The same was shown in cellular experiments with 2′,7′-dichlorofluorescein diacetate. The cytotoxicity of the compounds was studied on three cell lines: A549 (human lung adenocarcinoma), A549/DDP (cisplatin-resistant A549), and SKOV-3 (human ovarian cystadenocarcinoma). The toxicity of compound **6** was shown to be higher than that of compound **7** due to the factors of photocatalysis and generation of ROS. The most significant phototherapeutic index (PI) change was shown with the A549 cell line, where the PI was found to be 3 for complex **6** and 44 for complex **7**. The authors demonstrated similar outcomes using SKOV-3 3D multicellular spheroids. As a result, the biological activity of the compounds was investigated, demonstrating their applicability through several biological assays.

The next large subgroup of compounds **8–18** was obtained in the laboratories of Gazer and of Kodanko, who devoted their attention to inhibitors of the cytochrome P450 family. Cytochrome P450s are vital enzymes responsible for facilitating complex organic transformations crucial for the biosynthesis and metabolism of key molecules such as steroids, retinoic acid, and vitamin D. Compounds **8–10** were synthesized by Glazer *et al.* (Fig. 5).[33] These complexes exhibited absorption capabilities extending up to 600 nm with a maximum near 560 nm. The authors did not quantitatively estimate the quantum yields of singlet oxygen but showed that its generation is comparatively lower than for the same complex with three

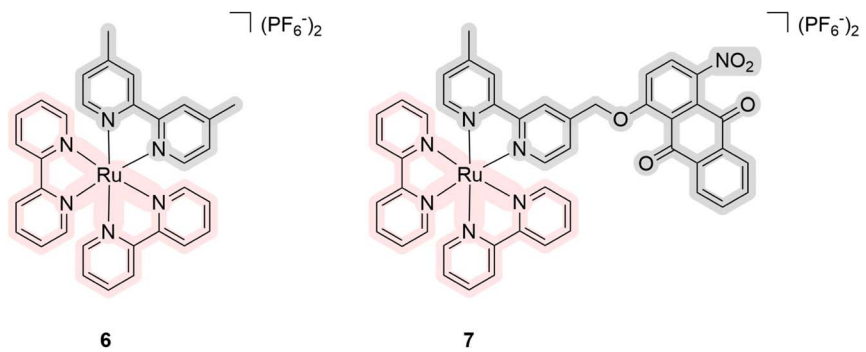

6 7

Fig. 4 Structures of ruthenium complexes **6** and **7** as multifunctional agents that exhibit properties of PDT/PACT agents. Light pink highlights a part of PS, while gray indicates the released ligand.

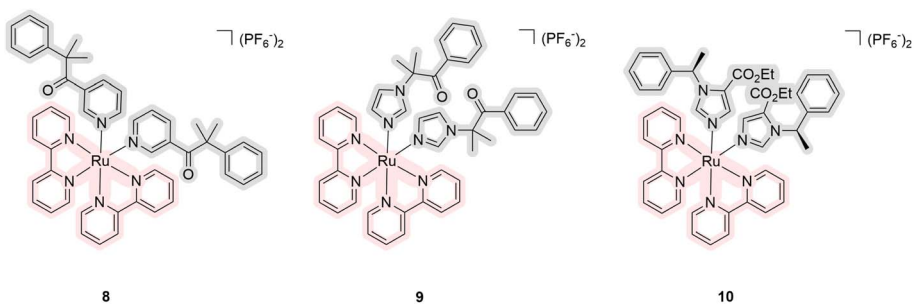

8 9 10

Fig. 5 Structures of ruthenium complexes **8–10** as prodrugs of inhibitors of the cytochrome that exhibit properties of PDT/PACT agents. Light pink highlights a part of PS, while gray indicates the released ligand.

bathophenanthroline ligands. A fluorescent substrate selective to the cytochrome P450 was used to demonstrate a 136-fold difference between intact and irradiated samples with IC_{50} values for enzyme inhibition of 6.8 and 0.05 μM, respectively. The cytotoxicity of the metal complexes after light irradiation was found to be comparable to the toxicity of released drugs. Using human liver microsomes, the authors demonstrated the ability of compound **9** to inhibit cytochrome P450 activity. At the same time, this compound was used to treat plasmids coding for green fluorescent protein in the presence and the absence of cytochrome to better visualize the difference in activity. The compound was found to be toxic under light irradiation due to DNA intercalation of the Ru(II) center as there was no influence of cytochrome. It means that *in vitro* experiments have confirmed that the Ru(II) center can target DNA, while the released ligands target the P450 enzyme. This suggests that the compounds have toxicity not only because of the ligand released as a chemotherapeutic agent but also because the released ruthenium itself may chemically interact with the environment after the loss of the ligand.

In 2021, another series of ruthenium complexes as photocages for cytochrome P450 inhibitors were obtained by Kodanko *et al.* (Fig. 6).[34] Complexes **11–15** contain an octahedral ruthenium complex as a core responsible for singlet oxygen generation and a pyridine-coordinated ligand that is released under light irradiation. These pyridine ligands are analogs of the antiretroviral drug ritonavir, which is a CYP3A4 inhibitor. Compounds **11** and **13** showed no generation of singlet oxygen before and after the release in methanol, while the others have values of quantum yields of singlet oxygen of 57–80%. The quantum yields of photosubstitution measured in acetonitrile are in the range of 1.4–6.1%. The maximum absorption lies near 470 nm and the tail of the absorption spectrum is up to 600 nm in acetonitrile. The PI for the compounds ranged from 0.3 to 2.3 based on studies of half-maximal inhibitory concentration (IC_{50}). The biological studies were performed using a human adenocarcinoma cell line DU-145, which is known to have high levels of cytochrome P450 expression. The drug vinblastine, which had previously shown synergy with cytochrome P450 inhibitors, was used to increase the efficacy of the drugs. Compound **12** showed the highest toxicity under light irradiation (EC_{50} = 2.8 μM) in contrast to the sample in the dark (EC_{50} > 25 μM). The authors demonstrated that inhibition can be enhanced by a drug release strategy, as metal complexes in cells can bind tightly and selectively to the active site of cytochrome P450s without heme ligation.

The next series of ruthenium complexes comprises the compounds obtained in 2022 by the Glazer group (Scheme 1).[35] Similarly to the previous series, complexes **16–18** include ligands that serve as inhibitors of one protein from the CYP1B1 family of P450 cytochromes. CYP19A1 was targeted because it produces estrogen and thus provides fuel for estrogen-induced cancers. Tetramethoxystilbene was chosen as a ligand because several derivatives could be obtained if necessary to establish selectivity. The resulting complexes do not generate singlet oxygen according to the Singlet Oxygen Sensor Green assay but showed low levels of ROS generation. The quantum yield of photosubstitution in 5% DMSO in water varied from 0.04% to

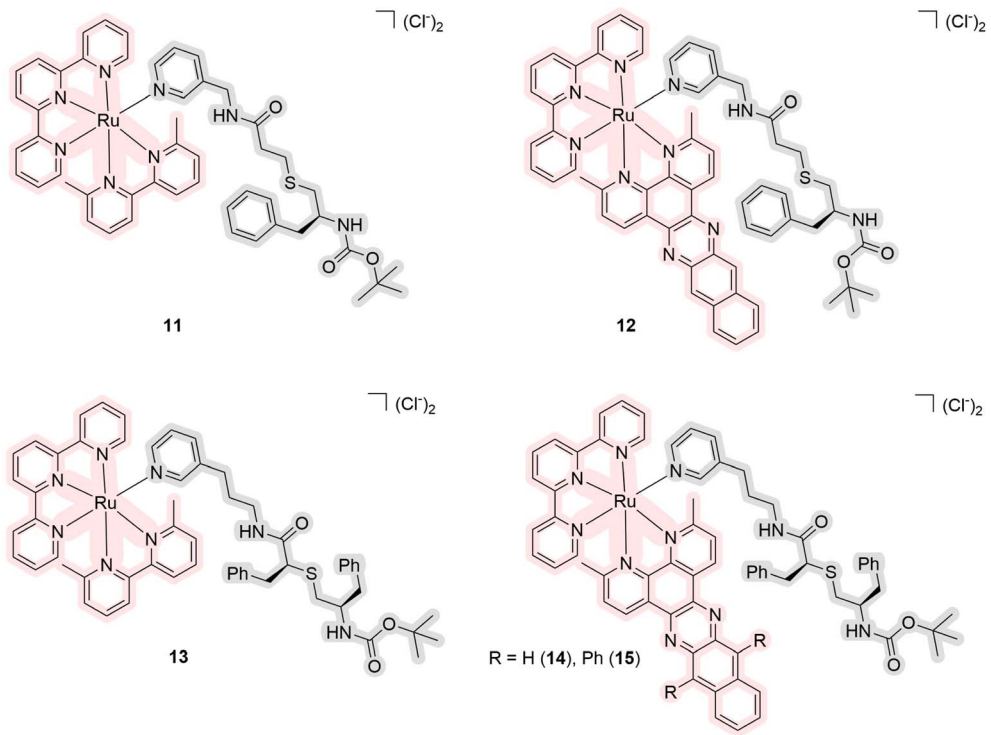

Fig. 6 Structures of ruthenium complexes **11–15** as prodrugs of inhibitors of the cytochrome that exhibit properties of PDT/PACT agents. Light pink indicates the part responsible for PDT, while gray indicates the released ligand.

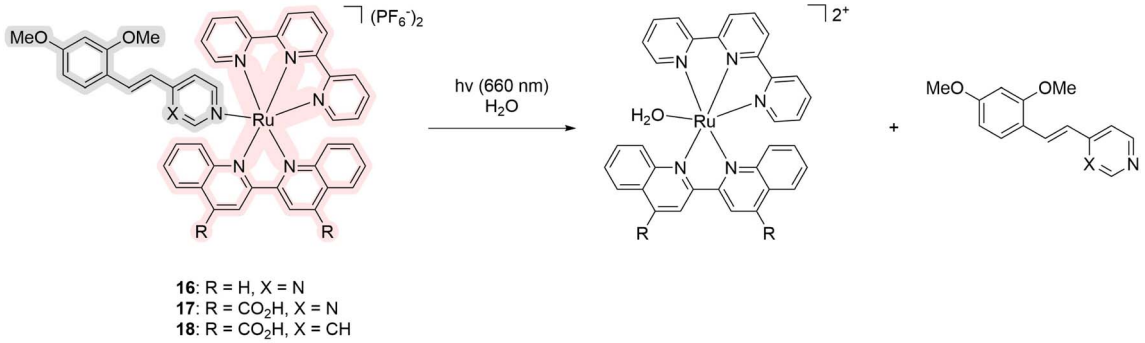

16: R = H, X = N
17: R = CO_2H, X = N
18: R = CO_2H, X = CH

Scheme 1 Scheme of the photorelease mechanism of ruthenium complexes **16–18** as prodrugs of inhibitors of the cytochrome that exhibit properties of PDT/PACT agents. Light pink highlights a part of PS, while gray indicates the released ligand.

5.5% depending on the structure. The compounds have an absorption maximum in water around 390, 455, and 550 nm, respectively. However, due to the extent of the tail of the spectrum, the authors studied the inhibition ability of the compounds upon irradiation at 660 nm. Complex **18** showed the highest PI values for CYP1B1 inhibition compared to the other cytochromes CYP1A1 and CYP19A1. The selectivity ratio of CYP1B1 inhibition to the other two was >100 000 and 62 800, respectively. However, the authors emphasize that low PI values are a persistent problem for ruthenium complexes and dark IC_{50} values are usually in the μM range. The reasons for the selectivity were not found due to the difficulty of the studied compounds for docking. Moreover, the addition of a carboxylic acid substituent to the ligand (**16** and **17**) was shown to reduce the inhibition of the CYP1B1 enzyme by about 10-fold. Unfortunately, these compounds have not been tested *in vivo*. Overall, the authors obtained and characterized in detail ruthenium complexes capable of selective inhibition of CYP1B1.

The next subgroup of compounds comprises ruthenium complexes with sulfur-coordinated ligands. Often, such compounds have extremely low quantum yields of singlet oxygen production, or the yields for these compounds have not been reported.[12,13,37–39] One example of a metal complex that can be considered a PDT/PACT dual agent is compound **19** (Scheme 2). This metal complex absorbs up to 550 nm with an absorption maximum of around 400 nm in acetonitrile solution. A pure HPLC sample of the compound had a 3% singlet oxygen production quantum yield. This value is much lower than those of clinically used PSs.[14] The quantum yield of photosubstitution was measured by UV-vis spectroscopy and found to be 11.1% in acetonitrile solution under green light irradiation (541 nm). The authors note that 15 minutes is sufficient to achieve complete photosubstitution. Under photo-irradiation, the non-toxic 2-((methylthio)methyl)pyridine ligand is released together with a ruthenium-based cytotoxic photoproduct (Scheme 2). This complex can bind to biomolecules such as nuclear DNA. The photocytotoxicity of the metal complex has been studied using several biological assays. In *in vitro* experiments using the cell lines A549 (human lung adenocarcinoma), PC3Pro4 (human prostate carcinoma), CRMM1, CRMM2, and CM2005.1 (three lines of conjunctival melanoma), and OMM1, OMM2.5, and MEL270 (three lines of uveal melanoma), metal complex **19** showed high PI values up to 31 (PC3Pro4 cell line). However, in *in vivo* experiments, the compound was not as efficient against implanted PC3Pro4 cells as against CRMM1 and CRMM2. The latter showed lower PI values *in vitro*. The authors conclude that this demonstrates the difficulty in the translation of *in vitro* cytotoxicity results to an *in vivo* model. Overall, the resulting metal complex is a rare example of a dual agent that has shown efficacy in both *in vivo* and *in vivo* models.

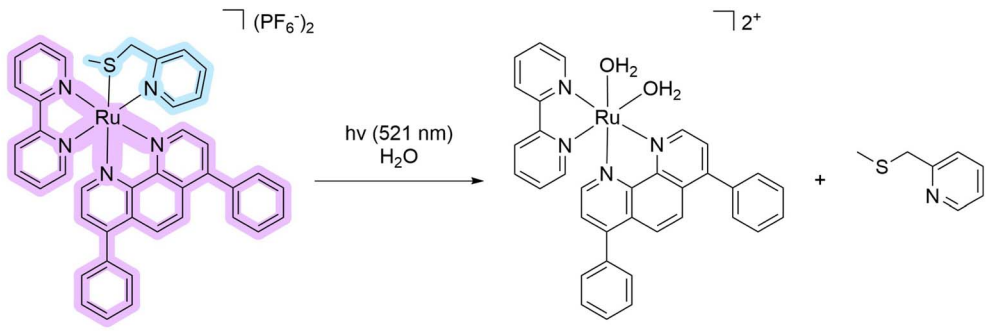

19

Scheme 2 Scheme of the photorelease mechanism of ruthenium complex **19** as a prodrug of a toxic ruthenium aqua-complex that exhibits properties of PDT/PACT agents. Light purple highlights a part of PS, while blue indicates the released ligand.

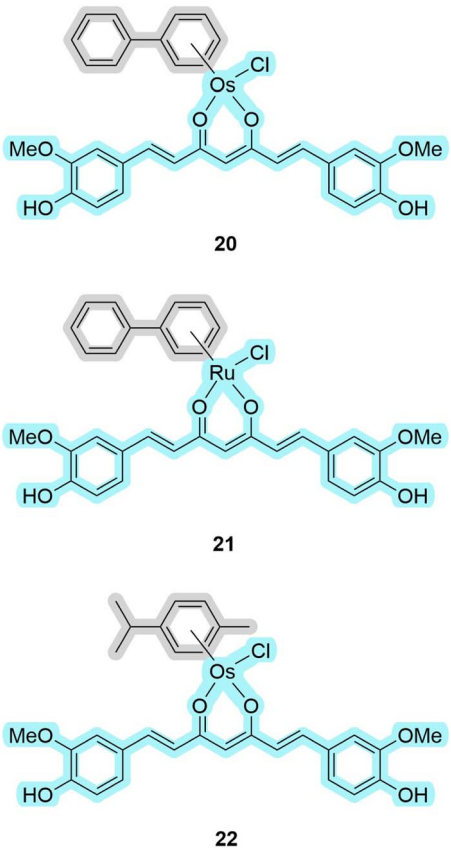

Fig. 7 Structures of osmium and ruthenium complexes **20**–**22** that exhibit properties of PDT/PACT agents. Light blue indicates the part responsible for PDT, while gray indicates the released ligand.

2.2. Osmium complexes

The photochemistry of osmium complexes has been less studied in comparison with ruthenium but their polypyridine complexes have proven to be quite promising PSs.[49–53] In 2021, the Sadler group reported the synthesis and evaluation of several osmium arene and ruthenium arene complexes with curcumin ligands (**20**–**22**, Fig. 7) that showed good anticancer potency.[54] These compounds absorb light in the visible region of 400–500 nm in phosphate-buffered saline (PBS). The authors did not mention the measurement of singlet oxygen production quantum yield, but the generation of ROS by complex **20** was confirmed using 2′,7′-dichlorofluorescein diacetate as a fluorescent ROS probe in cellular studies. Simultaneously, the authors were able to observe a gradual increase of the aromatic ligand concentration in the mixture upon photo-irradiation of the complexes, which confirmed the release of the ligand. Moreover, a change in the oxidation state of diamagnetic Os^{2+} to paramagnetic Os^{3+} was monitored by NMR. Various cell lines for the studies included A549 (human lung adenocarcinoma), A549R (cisplatin-resistant human lung adenocarcinoma), HeLa (human cervical adenocarcinoma), HepG2 (human liver carcinoma), HLF (human normal lung), and LO2 (normal liver). Osmium complex **20** showed higher PI values than **21**, **22**, curcumin alone, or cisplatin in all experiments performed. The highest PI value of 34.3 was observed for this metal complex in experiments with A549R, which makes it a promising agent for further studies. It was also found that photo-irradiation changes the localization of metal complexes from the mitochondria to the nucleus, resulting in mitochondrial damage, apoptosis, DNA damage, angiogenesis inhibition, and colony formation. The authors suggest that these processes might be related to the changes in the oxidation state of osmium. Overall, this work proposes a new strategy for designing multimodal anticancer drugs that can release an arene ligand and undergo oxidation of the metal centre upon irradiation.

2.3. Iridium complexes

In recent years, iridium has also witnessed a tremendous increase in interest for the development of PSs suitable for PDT.[55,56] To date, only a small number of iridium complexes having the properties of dual PDT/PACTs agent are known. Mao *et al.* reported cyclometallated complexes **23**–**25** (Fig. 8), which can release their five-membered ring ligands (an imidazole or a pyrazole) under photo-irradiation, as promising dual agents with high phototoxicity values.[57] These compounds have an absorption maximum of around 260 nm with a tail of up to 450 nm in dichloromethane solution. They have high singlet oxygen production quantum yields of 79–86% as evaluated using the indicator 1,3-diphenylisobenzofuran in methanol. The quantum yields of photorelease were not evaluated, but it was noted that the emission intensity of the metal complexes drops by 20% when irradiated with blue light for 10 minutes in

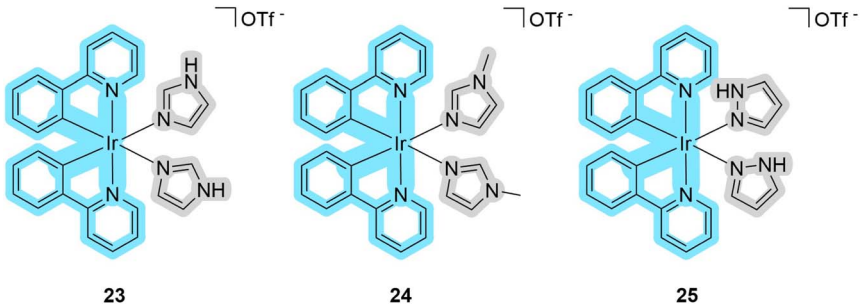

Fig. 8 Structures of iridium complexes **23**–**25** that exhibit properties of PDT/PACT agents. Blue indicates the part responsible for PDT, while gray indicates the released ligand.

phosphate-buffered saline. Studies with the indicator 2′,7′-dichlorofluorescein on the A549 cell line confirmed the intracellular generation of ROS by flow cytometry. For the biological experiments, the authors used a variety of cell lines: A549 (human lung adenocarcinoma), A549R (cisplatin-resistant human lung adenocarcinoma), PC3 (human prostatic adenocarcinoma), HepG2 (human liver carcinoma), and LO2 (normal liver). **23** and **25** showed higher PI values compared to compound **24**. The maximum value of PI equal to 61.7 was measured for metal complex **23** against the HepG2 cell line. The authors not only studied the localization of the metal complexes, which are predominantly in the cytoplasm, but also demonstrated that the compounds can covalently link to biomolecules after photodissociation by complexing to histidine residues in proteins.

An original strategy to overcome hypoxia was devised by the groups of Chao and Gasser in 2022. The idea was to merge two strategies: directly deliver oxygen-carrying compounds, endoperoxides, to the hypoxic tumor to increase the efficacy of Type II PDT treatment that requires oxygen,[58–60] and under photoirradiation generate carbon radicals as photoactivated toxic species.[61] Thus, the following compounds **26–27** have been proposed and synthesized following these ideas (Fig. 9).[62]

These metal complexes absorb up to 450 nm with a maximum of around 300 nm in methanol. The quantum yields of photorelease were not measured, but the authors estimated an 80% photoconversion in 2 min at 405 nm in DMSO solution under hypoxic conditions (1% oxygen). The quantum yields of singlet oxygen production were found to be 79% for complex **26** and 16% for **27**. Based on the results of the HPLC-MS analysis and EPR, the following scheme of phototransformation was suggested (Scheme 3). Under light irradiation, the iridium complex releases a highly cytotoxic iridium complex, singlet oxygen, and an alkoxy radical. Due to the high generation of ROS, complex **26** was selected for further *in vitro* studies on the A549 (human lung adenocarcinoma) cell line. Under hypoxic conditions (1% oxygen), the PI of compound **26** was 690, whereas under normoxic conditions (21% oxygen) it was 959. The iridium complex, which is a photoreleasing product of metal complex **26**, was found to be highly toxic. The authors were also able to show the release of the compound intracellularly using lifetime phosphorescence imaging. Microscopic images showed signs of cellular damage, including a reduction in mitochondrial size and the formation of vesicles within the cell after the photorelease. Using two-photon excitation of A549 multicellular tumor spheroids by confocal microscopy, it was demonstrated that all layers of cancer cells could be treated efficiently with metal complex **26**. Further, *in vivo* studies with the encapsulation of **26** in phospholipids were performed on A549 tumor-bearing Nu mice. It was found that the formed nanoparticles almost completely eradicated the tumor in a mouse model under two-photon irradiation (750 nm). Overall, the obtained compound **26** is one of the most

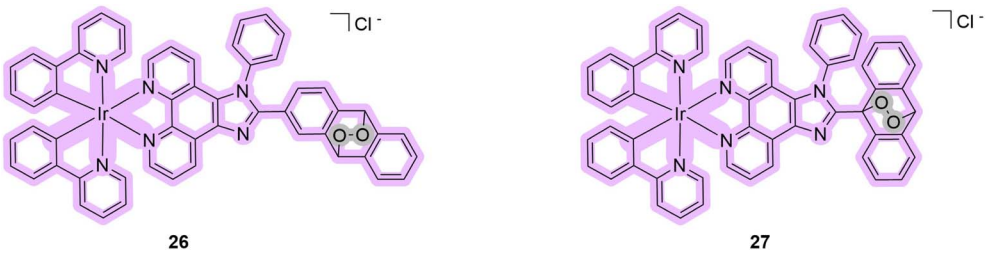

Fig. 9 Structures of iridium complexes **26–27** that exhibit properties of PDT/PACT agents. Purple indicates the part responsible for PDT, while gray indicates the released oxygen.

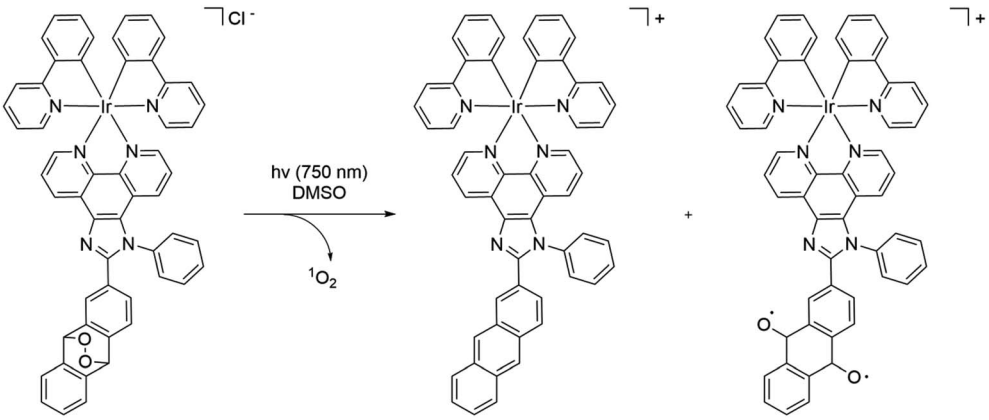

Scheme 3 Scheme of the photorelease mechanism of ruthenium complex **26** as a prodrug of singlet oxygen, a toxic complex, and an alkoxy radical that exhibits properties of PDT/PACT agents.

effective metal-based PDT PSs that can be used under hypoxic conditions with two-photon excitation.

2.4. Binuclear complexes

Some of the most attractive molecules are those in which different parts of the molecule are responsible for PDT and PACT properties.[11,63] Among the compounds that have been reported in the literature, the Ru–Ir compound **28** is a unique binuclear complex where the iridium subunit serves as a PS, and the ruthenium one as a drug photoreleasing moiety (Scheme 4).[11] The authors wanted to obtain the binuclear complex as a mitochondria-targeting compound to treat platinum-resistant cell lines.[64] The compound in phosphate-buffered saline had absorption bands around 380–405 nm and 450 nm. The release of the ruthenium complex was confirmed by NMR spectroscopy, absorption spectroscopy, and HPLC. The last method allowed authors to identify the degradation products (Scheme 4). The quantum yield of singlet oxygen of the compound under 405 nm irradiation was 46% in studies with methylene blue as a standard in methanol solution. However, at 450 nm irradiation, the complex does not generate singlet oxygen, and thus 405 nm was utilized for cellular experiments. Four cell lines were tested: two *cis*-platinum resistant/two non-cisplatin resistant cell lines A549/A549R (human lung adenocarcinoma) and SGC-7901/SGC-7901DDP (human gastric adenocarcinoma). With A549R, the compound demonstrated higher cytotoxicity ($IC_{50} = 11.34 \pm 1.2$ μM) without light irradiation in comparison with cisplatin ($IC_{50} = 92.54 \pm 9.2$ μM). Upon photo-irradiation, the toxicity increased to $IC_{50} = 0.45 \pm 0.1$ μM. Thus, the PI value was found to be 25.2 for the promising dual agent. The same pattern of changes was observed for other cell lines. In contrast to previous studies, the authors were able to demonstrate the ability of the released ruthenium complex to bind to DNA. For this purpose, the authors used a gel electrophoresis assay with the plasmid pBR322. After light irradiation of the complex in the presence of the plasmid, a delayed shift was observed by electrophoreses that demonstrated the binding ability of the ruthenium-releasing moiety. The ability of the compounds to induce mitochondrial dysfunction due to DNA damage was also demonstrated, which was characterized by a decrease in the level of adenosine triphosphate (ATP). Overall, the authors showed the possibility of using the dual agent as an effective PS capable of inducing mitochondrial stress through the release of the ruthenium complex.

3. Organic compounds as PSs

Among organic-based PSs used as PDT/PACT agents, two main groups emerge: 4,4-difluoro-4-bora-3*a*,4*a*-diaza-*s*-indacene (BODIPY) and polypyrrole macrocycles. BODIPY compounds gained attention due to their use as dyes for bioimaging, broad spectral characteristics, and high luminescence quantum yields.[65,66] Polypyrrole macrocycles like silicon phthalocyanines and porphyrins are also known in the literature to exhibit properties as PDT/PACT agents. The interest in these compounds is linked to their application in PDT as effective PSs.[67,68] We report below first examples of BODIPYs and then phthalocyanines, as well as other examples based on organic PSs as dual PDT/PACT agents.

3.1. BODIPYs

The second broadest class of compounds after ruthenium complexes that can serve as PDT/PACT agents are BODIPY

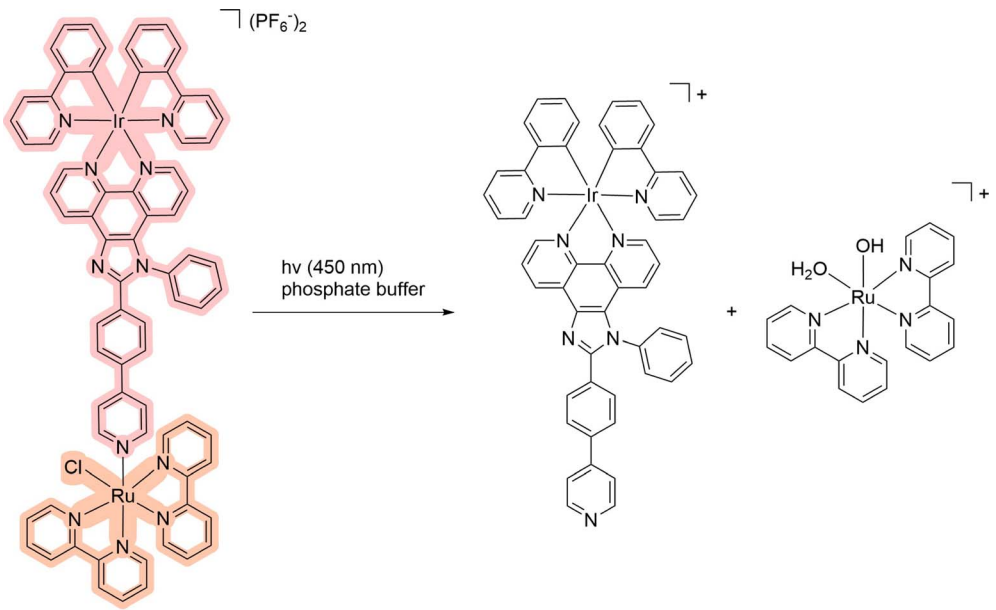

28

Scheme 4 Scheme of the photorelease mechanism of the binuclear complex **28** that exhibits properties of PDT/PACT agents. Light red highlights the PS, while orange indicates the compound released.

compounds. The greatest contribution to the field of study of these compounds as possible PACT agents comes from the groups of Winter and Weinstain.[66,69,70] In their joint review in 2023, they combined the most significant trends in the variation of photophysical properties depending on (1) the structure of the BODIPY backbone, (2) the nature of the leaving group, and (3) the substituents at the boron.[66] It should be noted that this review considers exclusively the meso-position in the structure as a bridge between the molecule and the leaving group (Scheme 5). An earlier Weinstain review from 2020 showed that the photodegradation process is observed at the position where the electron density decreases when the substance is irradiated with light.[28] In the case of BODIPY compounds, it is in the meso-position of the molecule backbone that the electron density decreases the most.[66] An in-depth explanation of the mechanism of photorelease has been theoretically studied.[66,71]

Among the compounds that can be found in the literature exhibiting the properties of PDT/PACT agents are the molecules shown in Fig. 10.[63,72–74]

In the case of **29–34**, the PS is BODIPY itself. It serves also as a photocage. The exact mechanism of photorelease from BODIPY meso-methyl remains unknown but has been proposed to be a photo-S_N1 type mechanism.[66] Under photo-irradiation, the molecule reaches a higher-lying singlet excited state. Calculations suggest that the molecule degrades from this state, leading to the formation of a putative carbocation and a leaving group (Scheme 6). In the presence of methanol, a methoxy derivative is formed. Compound **29** includes a derivative of chlorambucil, which has shown efficacy in anticancer chemotherapy.[75] The compound exhibits absorption up to 600 nm with a maximum at 550 nm in phosphate-buffered saline. The complete release of chlorambucil was observed upon 1 h irradiation at 561 nm. The starting BODIPY with a hydroxy substituent has a singlet oxygen quantum yield of 55%, while the resulting product has a quantum yield of 21% in acetonitrile solution. Cytotoxicity investigations on HeLa (human cervical adenocarcinoma) revealed relatively low toxicity for the complex, with 75% of surviving cells when incubated with 50 μM for 24 h in the dark. Under light irradiation, the cell survival rate dropped below 40% after 15 minutes and nearly reached zero after 1 h. Moreover, at equal concentrations, the BODIPY compound exhibited higher cytotoxicity compared to chlorambucil, likely attributed to the generation of singlet oxygen and the enhancement of phototoxicity.

The described compound includes an ester bond as a linker between the backbone of the molecule and the leaving group. Such a bond can be often enzymatically broken by esterases.[76,77] While compound **29** was not investigated for stability to esterases, compounds **30–32** were.[74] Compounds **30–32** include a fragment of the cysteine protease cathepsin B inhibitor with a broad scope of functions.[78,79] The authors tried to overcome resistance to esterases by varying the nature of substituents, which succeeded for **31** (Fig. 10). All compounds absorb light in the 400–550 nm range with a maximum of around 525 nm in

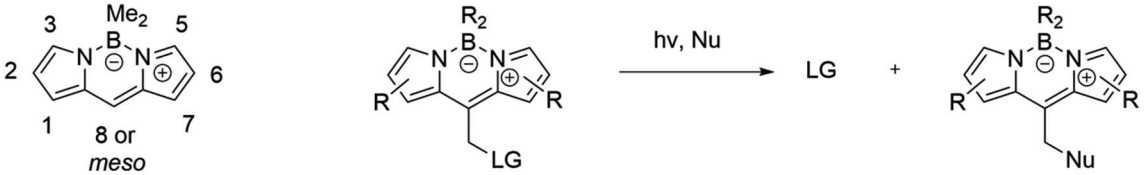

Scheme 5 General mechanism of photoconversion of BODIPYs into by-products and released drugs. LG – leaving group that in the observed cases is the drug and Nu – a nucleophile, usually solvent molecules. The overall mechanism may not correspond to all examples of photorelease.

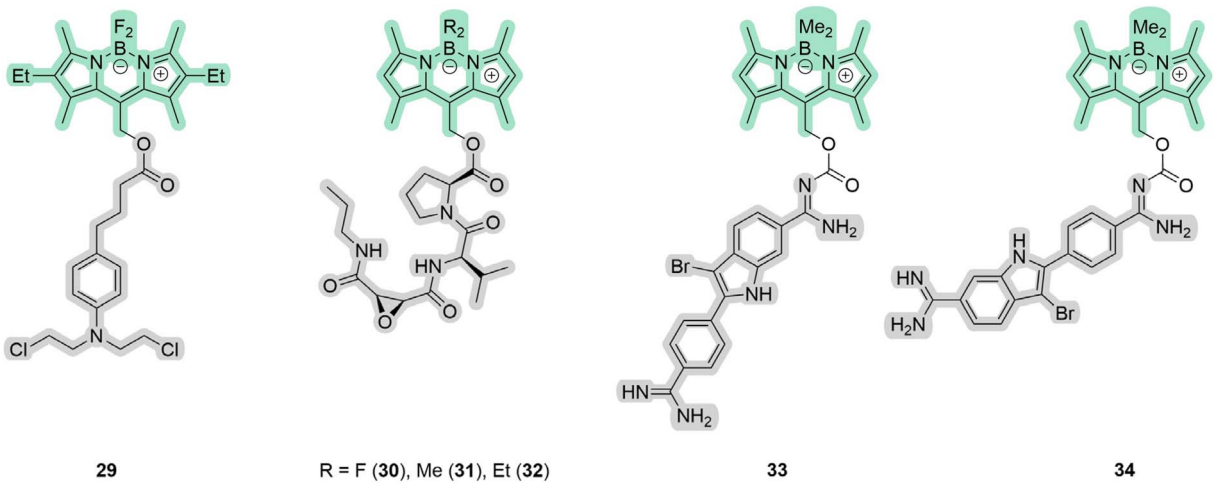

29 R = F (**30**), Me (**31**), Et (**32**) 33 34

Fig. 10 Structures of BODIPYs **29–34** that exhibit properties of PDT/PACT agents. Green highlights the PS, while gray indicates the compound released.

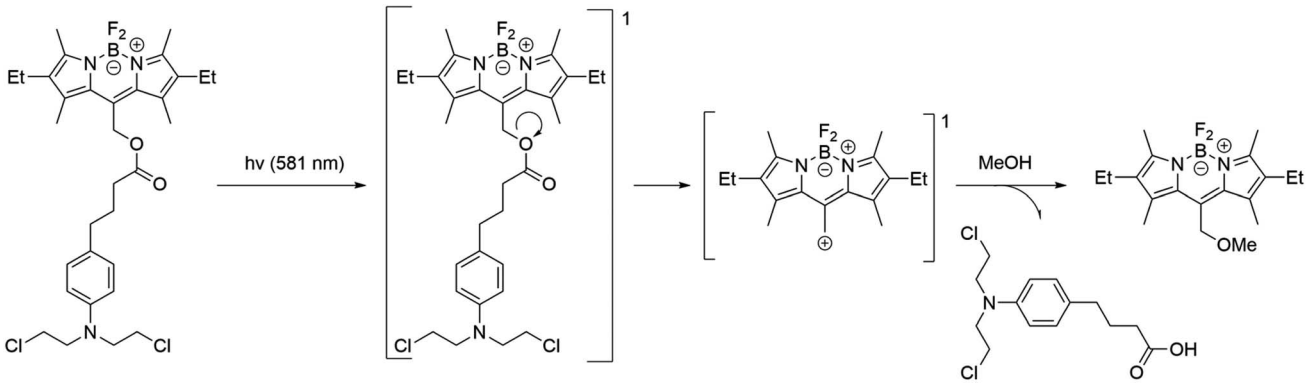

Scheme 6 Scheme of the photorelease mechanism for compound **29**. 1 indicates a singlet state.

dichloromethane. The quantum yield of photorelease was approximately 2.5% for compound **31** in methanol. The quantum yield of singlet oxygen was determined relative to methylene blue using 1,2-diphenylisobenzofuran in isopropyl alcohol, with complex **31** having the highest value. MDA-MB-231 (human breast carcinoma) and MCF-10A (human normal epithelial) cell lines were used to evaluate cytotoxicity. The compounds are non-toxic without light irradiation. The PI values were found to be 30 for the cancerous line and 7.7 for the non-tumorigenic one, showing the selectivity of the drug. As a result, the authors showed that the combination of rapid and selective inactivation of Cathepsin B with singlet oxygen generation results in a synergistic effect that steers cancer cells away from apoptotic death in favor of necrosis.

In the case of **33–34**, the authors obtained compounds consisting of a BODIPY residue and a leaving group with a carbamate bond. Under light irradiation, a DNA-binding PS is released, namely Br-DAPI (highlighted in gray in **33**, **34**), and generates carbon dioxide.[73] As in the previous case, the authors used the so-called photocage WinterGreen. The carbamate linker was chosen because of the higher quantum yield of photorelease compared to the direct nitrogen–carbon bond.[80] Similarly to the previous example, the compounds have absorption maxima around 320 and 520 nm in PBS. After 20 minutes of 480 nm irradiation, the drug was completely released in the same buffer. However, no boron-containing release products were found in the sample due to photobleaching. The quantum yield of singlet oxygen was found to be 0.42% in aqueous ethanol solution. MCF7 (human breast carcinoma), A549 (human lung adenocarcinoma), and HeLa (human cervical adenocarcinoma) lines were used to estimate the toxicity of the compounds. No enzymatic cleavage occurred after the incubation of the compounds with cells in the dark, without light irradiation. Also, in the dark, Br-DAPI compared with **33** showed different cytotoxicity depending on the cell line, which may be due to cell permeability and defense mechanisms against oxidative stress. The toxicity of the compounds was estimated as the concentration that reduces the number of viable cells by 50% (CC_{50}) in the dark and under light irradiation. We calculated PI values based on the data presented in the paper. In the case of the MCF7 line when UV + 480 nm was applied, the PI was approximately 26 for **33** and 21 for **34**. The PIs were lower when only 480 nm was used, which was explained by the lower ROS generation. This is also explained by the spectral separation of BODIPY (480 nm) and Br-DAPI (UV) photorelease activation. In summary, the authors have shown that the use of **34** drugs is preferable due to the achievement of high levels of phototoxicity due to the dual PDT/PACT treatment.

3.2. Silicon phthalocyanines

These compounds share a release mechanism similar to ruthenium complexes. Upon light excitation, one of the ligands undergoes decoordination.[81] The released ligand serves as the drug. Significant contributions to the development of the chemistry of PDT/PACT agents have been made by You *et al.* Some of the first studies confirmed that aminoacrylate linkers can be cleaved in the presence of singlet oxygen.[82,83] Among these compounds, two have cleavable (**35** and **37**) and two stable linkers (**36** and **38**) to singlet oxygen (Fig. 11 and Scheme 7).[84,85] The connected drugs are FDA-approved tubulin polymerization inhibitors: combretastatin A4 and paclitaxel.[86,87] It was shown that absorption spectra, as well as emission spectra (**37** and **38**), do not change significantly due to the variation of substituents. The authors are more focused on the biological properties of the molecules, referring to the known photophysical characteristics of phthalocyanines as effective PSs for singlet oxygen generation.[88,89] Compounds **35** and **36** were embedded in poly(ethylene glycol)-poly(D,L-lactide) micelles. The size was chosen to allow the enhanced permeability and retention (EPR) effect. Notably, the authors investigated the bystander effect on the Colon-26 line (mice colorectal carcinoma). In their setup, they use 24-well plates in which one half of each well is concealed, so that only one half can be photo-irradiated. Irradiation can lead to the release of both singlet oxygen and drugs, but the toxicity of singlet oxygen remains localized in the irradiated half. Yet they could observe that toxicity occurs in the non-irradiated half as well. This phenomenon, known as the bystander effect, occurs because non-irradiated cells were affected by the released drug that diffused in the well. In this way, the authors confirmed the release of the drug as a main factor of toxicity. It was concluded

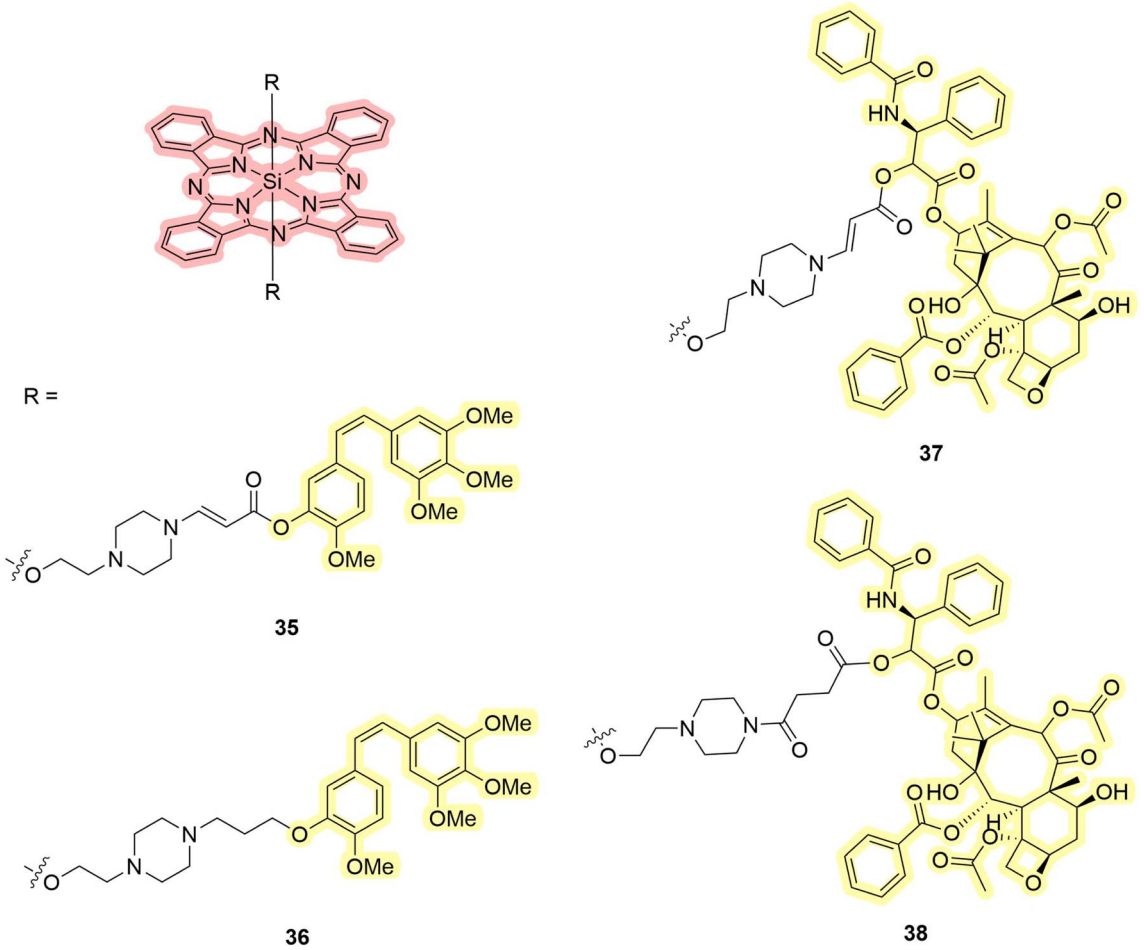

Fig. 11 Structures of silicon phthalocyanines **35**–**38** that exhibit properties of PDT/PACT agents. Red highlights the PS, while yellow indicates the compound released.

that despite the difference in linkers, compounds **35** and **36** showed toxicity upon light irradiation. The toxicity was higher for the compound with a cleavable linker in *in vivo* studies on BALB/c mice with single carcinoma tumors. Compounds **37** and **38** were used without incorporation into micelles. The toxicity of **37** and **38** was investigated using SKOV-3 cells (human

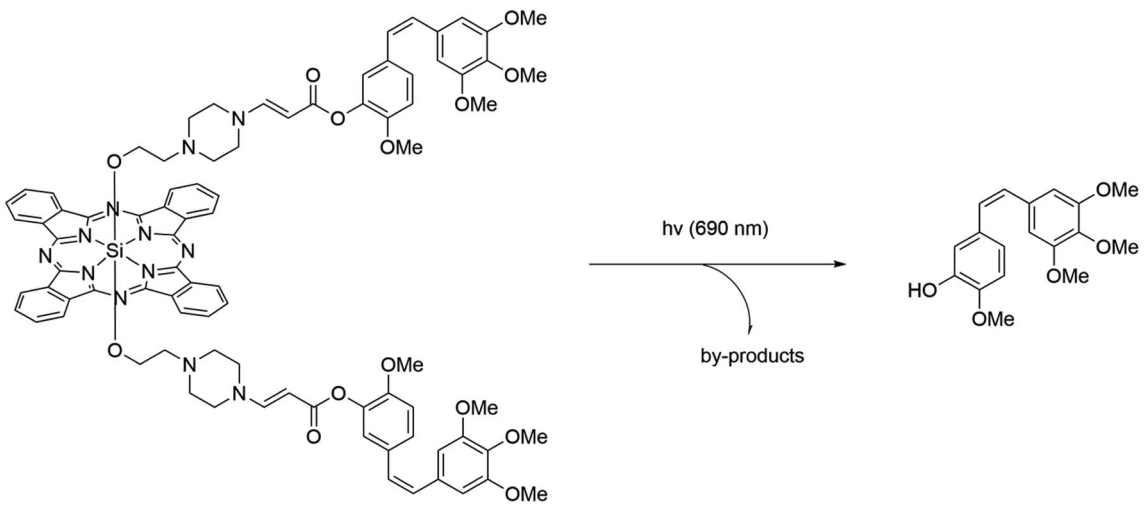

Scheme 7 Scheme of the photorelease mechanism for compound **35**.

ovarian cystadenocarcinoma). The drug itself showed high cytotoxicity against SKOV-3 cells with $IC_{50} = 4.7$ nM, while the compounds demonstrated lower toxicity: $IC_{50} = 910$ (**37**) and 1279 nM (**38**). After illumination, both showed strong cytotoxicity with $IC_{50} = 3.9$ and 24 nM, respectively. Thus, the authors have demonstrated highly cytotoxic compounds activated by light, with the cytotoxicity in the case of the stable linker being due to the ability of the PS and in the case of the cleavable linker being due to both PDT and PACT mechanisms.

Fig. 12 illustrates the structures of compounds **39–41** obtained by Schnermann *et al.*[90] Building upon prior research concerning the release of oxygen-coordinated compounds, the authors decided to explore the possibility of releasing ligands directly coordinated to silicon. Specifically, combretastatin A4 was serving as a releasing moiety within the structure **41**.[86] For the sake of comparison, the authors included a less active trans analog **40** and a fluorescent dye in the release study **39** (Scheme 8). The fluorescent dye released allowed *in situ* estimation of the photodissociation rate. All the compounds exhibited absorption peaks around 690 nm, with quantum yields of singlet oxygen ranging from 10% (**40**) to 39% (**39**) in phosphate-buffered saline. In the case of these molecules, the release process competes with triplet–triplet annihilation processes. Consequently, in the absence of oxygen, a preferential release is expected. This phenomenon was demonstrated for compounds **40** and **41**, where the presence of sulfur-containing ligands in the medium is a prerequisite. Compound **41** releases 56% of combretastatin A4 and 9% of its trans analog due to a change in stereochemistry. Experiments were additionally carried out on the HeLa cell line (human cervical adenocarcinoma), revealing the localization of compounds in lysosomes. In the absence of light, the compounds exhibited negligible cytotoxicity. However, upon light irradiation, compound **41** induced an 80% growth inhibition, comparable to the uncoordinated drug. The compounds have high quantum yields and absorption in the red region, which makes them one of the most promising among the considered groups of compounds.

3.3. Platinum complexes as drugs

Another group of compounds of interest platinum-based drugs in PDT/PACT agents (Fig. 13). To date, we have identified several examples of platinum-containing compounds. Significant contributions to the development of azido platinum(IV) complexes have been made by Sadler's group, as detailed in a recent review.[50] These compounds share a common concept: the platinum(IV) center is attached to an organic PS and the irradiation leads to the release of a platinum(II)-containing drug. This is in contrast with ruthenium-based agents, where the metal plays the role of a moiety of the PS.

The group of Yan described the platinum complex conjugate to chlorin e6 **42** as a potential agent for the anticancer treatment of hypoxic cells.[91] Chlorin e6 is a well-known PS certified by the FDA.[92] The choice of the platinum azide complex was justified by its inertness during storage and ease of activation with nitrogen release. The compound was used to co-assemble with upconversion nanoparticles. In this way, the authors overcame one of the main problems of PDT – the absorption of light by tissues in the visible range. It requires the absorption peak to be shifted towards the first transparency window (values vary, approximately 700–980 nm).[93,94] In this case, the compound absorbs around 980 nm in aqueous medium. Embedding in the nanocomposite material also prevented the spontaneous platinum(IV) to platinum(II) process in the presence of dithiothreitol, which is usually characteristic of platinum(IV) complexes. Due to the competition between the release and singlet oxygen generation processes, a non-linearity tendency in singlet oxygen generation was observed. The more platinum complex was released, the more energy went to chlorin e6. Nanocoatings were investigated *in vivo* and *in vitro*. The authors conducted experiments on HeLa (human cervical adenocarcinoma),

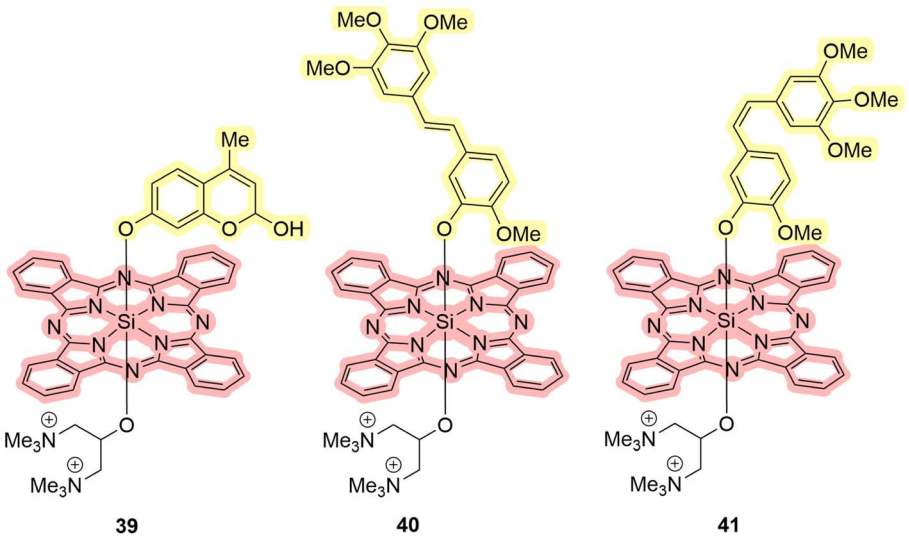

Fig. 12 Structures of silicon complexes **39–41** that exhibit properties of PDT/PACT agents. Red highlights the PS, while yellow indicates the compound released.

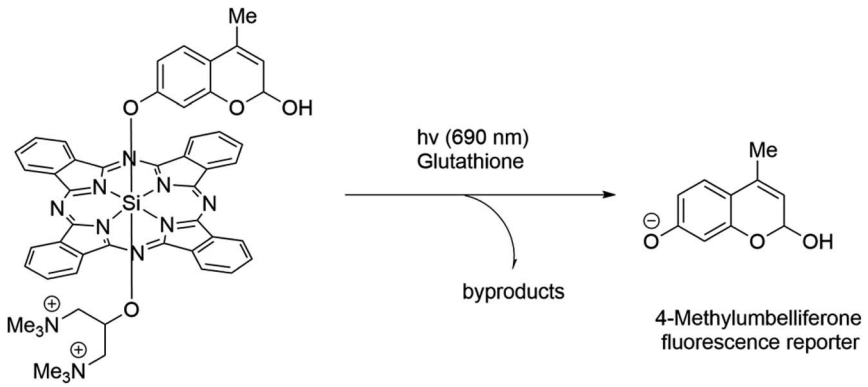

Scheme 8 Scheme of the photorelease mechanism for the compounds **39**.

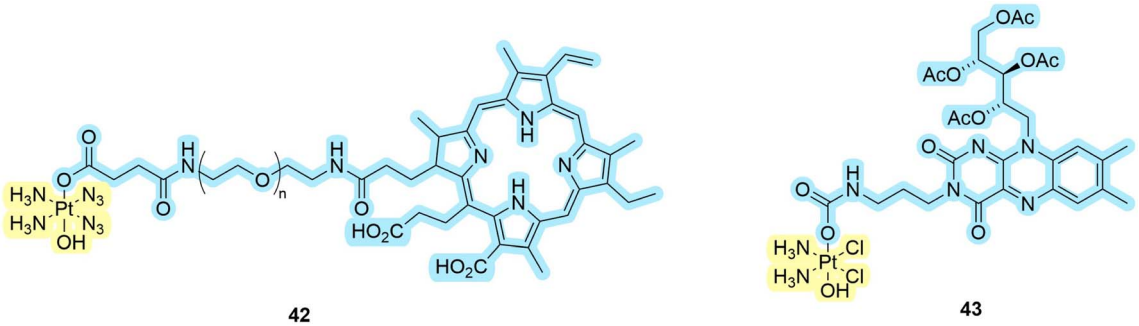

Fig. 13 Structures of platinum complexes **42–43** that exhibit properties of PDT/PACT. Blue highlights the PS, while light yellow indicates the compound released.

HCT116 (human colorectal carcinoma), MDA-MB-231 (human breast carcinoma), and B16 tumor-bearing mice to evaluate the antitumor activity. Treatment with the conjugate combined with near-infrared (NIR) irradiation resulted in a significant reduction in tumor growth compared to control groups. The authors also conducted studies using MDA-MB-231 cells to evaluate ROS levels and hypoxia-inducible factor (HIF-1α) expression under hypoxic conditions. The stabilization of HIFs under hypoxia leads to the transcriptional activation of genes involved in adapting cellular physiology to low oxygen levels. This includes promoting angiogenesis, glucose transport, and glycolytic metabolism.[17] Treatment with the conjugate resulted in increased ROS levels and reduced HIF-1α expression, suggesting that the conjugate can overcome hypoxia in tumors. Overall, the study suggests that the self-generating conjugate has the potential as an antitumor treatment for various types of tumors.

Beloglazkina *et al.* evaluated the applicability of compound **43** called riboplatin for biological purposes.[95] The drug was constructed with TARF (tetraacetylriboflavin, PS) and a platinum complex.[96,97] Upon light irradiation, the complex releases the drug through two mechanisms, dependent on whether it is in a triplet or singlet transition state (Scheme 9). In both cases, cisplatin is released. The authors determined that the compound has a 47% quantum yield of singlet oxygen in methanol. The absorption spectrum in contrast to the previous compound lies in the region down to 500 nm. Cytotoxicity studies showed that riboplatin was less toxic in the dark than cisplatin and led to better anticancer effects in MCF-7 human breast adenocarcinoma spheroids upon light irradiation. Moreover, it was found to be more efficient than the original TARF upon light irradiation. The authors express confidence in witnessing an increasing prevalence of platinum complexes as dual agents in the future, given the expanding pool of compounds demonstrating potential applicability in this domain.

3.4. Gold complexes as dual agents

Zou *et al.* recently synthesized complexes **44–46** to utilize gold(III) complexes exhibiting PDT/PACT properties (Fig. 14).[98] The complexes undergo photocatalytic activation to yield potent toxic gold(I) compounds. The necessary PS for this activation can originate from either the same complex or external photosensitizers. In their paper, the PS is a coordinated cyclometallated ligand, and the drug is a gold(I) compound itself. The compound obtained exhibited an absorption maximum of around 360 nm and a tail up to 420 nm in DMSO. Upon excitation at 420 nm in this solution, both the cyclometallated ligand and alkynyl ligands were released (Scheme 10). Simultaneously, the complex transformed into a gold(I) complex through the coordination of sulfur-containing ligands from the surroundings. It was shown that photoactivation with gold(I)

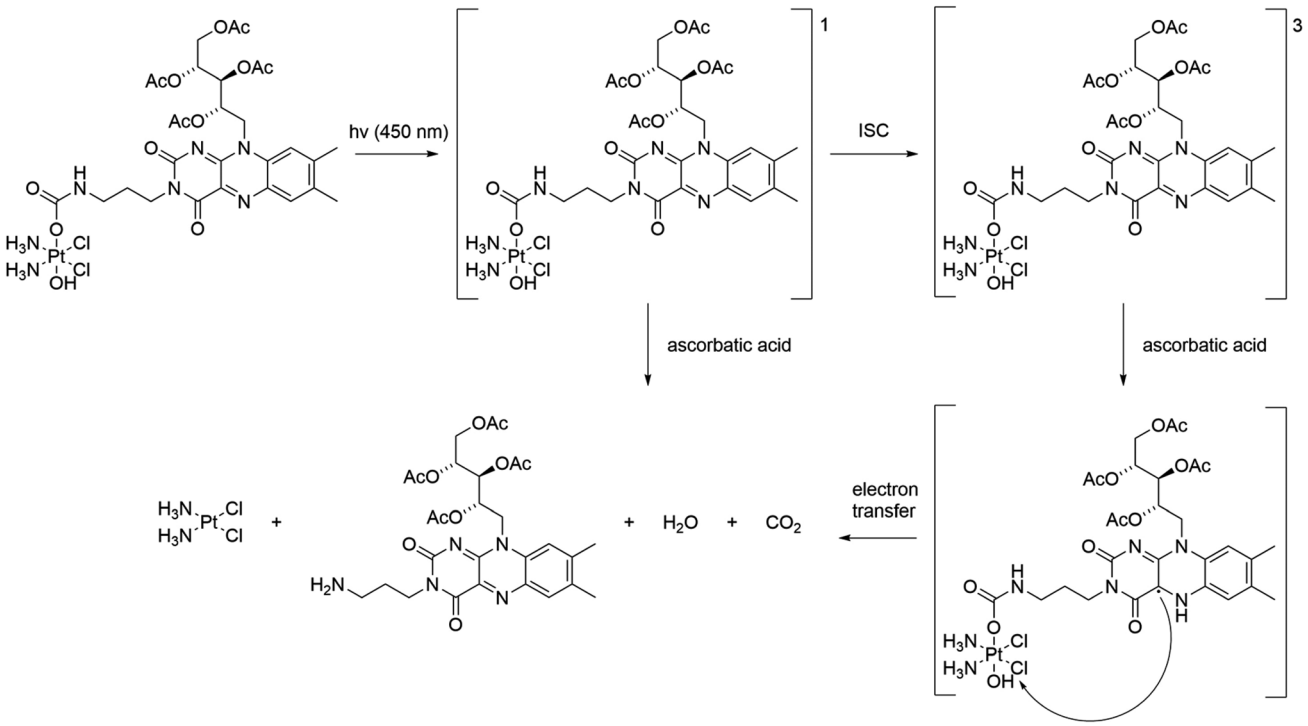

Scheme 9 Scheme of the photorelease mechanism for the compound **43**. 1 indicates the singlet state and 3 indicates the triplet state. ISC – intersystem crossing.

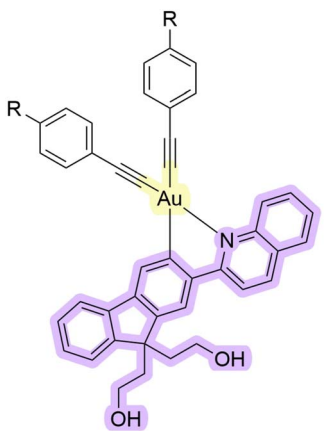

R = H (**44**), F (**45**), Me (**46**)

Fig. 14 Structures of gold complexes **44–46** that exhibit properties of PDT/PACT agents. Purple highlights the PS, while yellow indicates the releasing gold that serves as a toxic drug.

release is favoured under hypoxic conditions, while PS activation is favoured under normoxic conditions. The authors attributed the difference in the properties of the compound at different oxygen concentrations to the nature of the quenchers. Triplet oxygen is a stronger quencher of luminescence. Under normoxia, it quenches the emission faster than weaker quenchers like thiols. The authors determined the quantum yield of the photorelease to be 63% in DMSO upon 420 nm photo-irradiation, indicating a substantial level of photodegradation. Although the quantum yield of singlet oxygen was not measured, experiments with a fluorescent agent, Singlet Oxygen Sensor Green, confirmed its generation, revealing a significant formation of ROS under aerated conditions. *In vitro* and *in vivo* experiments were also performed. **44** caused potent photocytotoxicity after a short 5 minute irradiation with 420 nm light towards four different cancer human cell lines: A375 (human skin cancer), HCT116 (human colorectal carcinoma), A549 (human lung adenocarcinoma), and HepG2 (human liver carcinoma). IC_{50} values ranged from 0.47 to 1.0 μM with photo-irradiated cells and >100 μM with untreated cells. However, the non-cancerous liver cell LO2 (ref. 99) seems to be less susceptible to such photocytotoxicity with only a slight decrease in viability to 81.5%. Experiments with untreated zebrafish embryos showed no significant developmental changes. However, 630 nm irradiation with a combination of **44** and 5-aminolevulinic acid showed notable damage to blood vessels, particularly affecting the intersegmental vessel, dorsal longitudinal anastomotic vessel, and caudal vein. The authors demonstrated that gold complexes can be used for PDT/PACT purposes by conducting several biological studies that confirmed the applicability of the compounds under normoxic as well as under hypoxic conditions.

4. Comparison of photophysical and biological properties

To provide an overview of the compounds, we have summarised the photophysical data in regard to their biological properties of

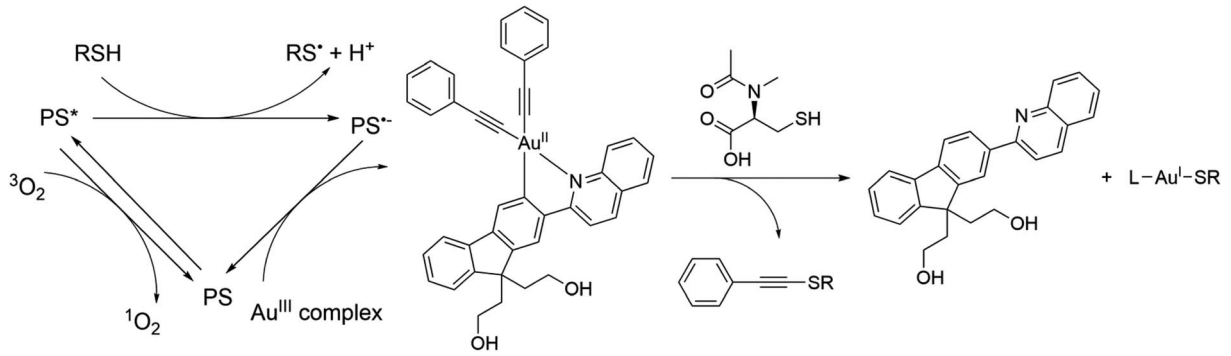

Scheme 10 Scheme of the photorelease mechanism for the compound **43**. PS is the photosensitizer and the Au^{III} complex is complex **43**. RSH indicates a thiol. L in the scheme indicates that the coordinated ligand may be different.

some representative dual agents in a single table, Table 1. The selection of compounds was made based on the availability of the necessary data to carry out a meaningful comparison.

To simplify the analysis, the values are considered sequentially from photophysical characteristics to biological properties. Among the compounds, most of them absorb in the visible range but in some cases the absorption maxima are close to the NIR. Earlier, we noted that the shift of absorption to this region is necessary because of tissue absorption of light in the visible range.[93,94] Quantum yields of singlet oxygen were not determined in all cases but the generation of it was confirmed using traps, luminescence spectra for the detection of the characteristic singlet oxygen peak, and other methods. In some cases, they are not presented due to the type of PS. For example, compounds **6** and **7** generate mostly ROS, *e.g.*, $O_2^{-\bullet}$ (Type I), and their quantum yield of singlet oxygen is low. Quantum yields of photorelease are labeled differently (Φ_λ, Φ_{LE}, Φ_{PS}, and Φ_{PD}) in articles but most studies use the same methods of actinometry[16,34,40,90,100] or chromatography[35,98] to quantify the value of photorelease. Comparing the quantum yields of drug release and the quantum yields of singlet oxygen, the latter is of greater magnitude. When energy dissipation pathways compete, singlet oxygen generation is likely to be favored; otherwise, the compound can be expected to be unstable.

Moving from photophysical to biological characteristics, we consider the changes in the toxicity of compounds analyzing EC_{50} and IC_{50}. These values are not suitable for comparing each compound from different series due to their dependence on cell incubation time,[74,101] irradiation time,[90,102] and even temperature during the irradiation period.[103,104] Therefore, within the scope of the comparison, we primarily compare the series as a whole to each other.

The first comparison factor is the toxicity of prodrugs and their drugs (**1** and **2**, NAMPT inhibitors; **12** and **14**, ritonavir derivatives; **28**, cisplatin; **37** and **38**, paclitaxel; **43**, cisplatin). Prodrugs are compounds that release drugs upon photo-irradiation. Comparing compounds **1** and **2** with the released NAMPT inhibitor, we observe a higher level of toxicity in the latter (*e.g.*, 20.6 and 45.6 μM *vs.* 10.8 μM). A similar comparison can be made between **37**, **38**, and paclitaxel (*e.g.*, 3.9 and 24 nM *vs.* 4.7 nM). In contrast, prodrugs **12**, **14** (*e.g.*, 2.8, >25 μM *vs.* >25 μM), **28** (*e.g.*, 6.4 μM *vs.* 10.3 μM), and **43** (*e.g.*, 32 μM *vs.* >200 μM) and their corresponding drugs show a different pattern where the toxicity of the drug is lower than the toxicity of the complexes. This can be explained by significant differences in solubility, charge, *etc.* between the neat drug and the complex. Overall, we do not observe uniformity in the change in cytotoxicity of neat drugs and their prodrugs.

The second comparison factor is the influence of the structure. When ruthenium complex pairs of derivatives **1** and **2** (*e.g.*, 20.6 μM *vs.* 45.6 μM), and **12** and **14** (*e.g.*, 2.8 μM *vs.* 25 μM) are compared, we note a significant contribution of the ligand structure of the compound to its toxicity. Examples **12** and **14** correspond to complexes with a change in the releasing ligand structure. **14** showed a higher PI (0.61) than **12** (0.30) in CYP3A4 inhibition tests *in vitro* but was less toxic to DU-145 cells *in vivo*. This is also a consequence of the difficult balance of PDT and PACT, as **12** is a more effective PS than **14** but has a lower quantum yield of photorelease. Overall, it demonstrates that the choice of a particular structure can have a significant impact on the efficacy of the dual agent.

The third factor is also structural. It is the choice of the nature of the releasing drug and PS. The effect of changing the releasing drug can be demonstrated by comparing BODIPYs **29**–**34**. Comparing their photophysical properties, we observe significantly different values of the quantum yields of photorelease (0.19–2.46%). This difference affects biological properties in the values of phototoxicity and hence PI (from 40 to 233). The prodrugs of similar platinum complexes **42** and **43** can be compared to demonstrate the changes when the nature of the whole PS is varied. The **43** complex releases in minutes, while **42** is capable of release in hours. As a result, we observe a significant contribution not only from the nature of the drug but also from the choice of the PS.

Considering these compounds, preference for certain types of drugs for certain PSs can be noted. For example, systems based on silicon phthalocyanines are favorable for oxygen-coordinated compounds, while ruthenium complexes are favorable for nitrogen-coordinated ones. Thus, varying the nature of the photocage and the drug it is worth keeping in mind more favoured combinations.

Table 1 Summary of the data of some of the discussed compounds: λ_{max} – absorption maxima; Φ_Δ – quantum yield of singlet oxygen; Φ_r – quantum yield of photorelease; EC_{50} – half-maximal effective concentration; IC_{50} – half-maximal inhibitory concentration; dark – without irradiation; light – with irradiation with the specified wavelength; N – normoxia; H – hypoxia; PI – Phototherapeutic Index. The symbol "∼" indicates an approximate number; * – authors used a Tokai Hit® stage top incubator; NAMPT inhibitor, ritonavir derivative, cisplatin, and paclitaxel are the drugs that are listed in the table after their prodrugs, *i.e.* molecules capable of releasing these drugs

Compound	λ_{max}, nm (ε, M^{-1} cm^{-1}, solvent)	Φ_Δ, % (λ, solvent)	Φ_r, % (λ, solvent)	EC_{50} or IC_{50} dark, μM (cell line)	EC_{50} or IC_{50} light, μM (λ, cell line)	PI
1	473 (8050, H_2O)	<0.5 (625, CD_3OD)	H: 5.8 (625, H_2O); N: 8.0 (625, H_2O)	H: 20.6; N: 8.9 (A549)	H: 17.9; N: 9.6 (visible*, A549)	H: 1.2; N: 0.93
2	531 (9320, H_2O)	3.6 (625, CD_3OD)	H: 1.3 (625, H_2O); N: 1.9 (625, H_2O)	H: 45.6; N: 20.3 (A549)	H: 18.7; N: 7.7 (visible*, A549)	H: 2.4; N: 2.6
NAMPT inhibitor	—	—	—	H: 10.8; N: 4.4 (A549)	N: 4.2 (visible*, A549)	—
6	560 (H_2O)	—	72 after 25 min (600, MeCN)	H: 33.9 ± 2.3; N: 36.2 ± 1.2 (A549)	H: 6.5 ± 0.5; N: 0.83 ± 0.02 (600, A549)	H: 5; N: 44
7	560 (H_2O)	—	47 after 25 min (600, MeCN)	H: 39.9 ± 3.1; N: 35.0 ± 2.1 (A549)	H: 15.6 ± 1.4; N: 11.2 ± 0.2 (600, A549)	H: 3; N: 3
12	∼490 (MeCN)	59 (460, MeOH)	2.4 (500, MeCN)	N: >25 (460, DU-145)	N: 2.8 ± 1.0 (DU-145)	—
14	∼490 (MeCN)	57 (460, MeOH)	1.4 (500, MeCN)	N: >25 (DU-145)	N: >25 (460, DU-145)	—
Ritonavir derivative	—	—	—	N: >25 (DU-145)	N: >25 (460, DU-145)	—
28	405 (15 680, PBS); 450 (7970, PBS)	46 (405, MeOH)	—	N: 6.4 ± 0.4 (A549) N: 11.3 ± 1.2 (A549R)	N: 1.8 ± 0.1 (450, A549) N: 0.5 ± 0.1 (405 + 450, A549) N: 1.0 ± 0.3 (450, A549R) N: 0.4 ± 0.1 (405 + 450, A549R)	A549: 3.5 (450); 12.2 (405 + 450) A549R: 11.6 (450); 25.2 (405 + 450)
Cisplatin	—	—	—	N: 10.3 ± 1.1 (A549) N: 92.5 ± 9.2 (A549R)	—	—
30	∼515 (DCM)	31.3 ± 8.8 relative to methylene blue (i-PrOH)	0.19 ± 0.02 (MeOH)	N: >50 (460–470, MDA-MB-231)	N: >50 (460–470, MDA-MB-231)	—
31	∼515 (DCM)	153 ± 35 relative to methylene blue (i-PrOH)	2.46 ± 0.19 (MeOH)	N: >100 (460−470, MDA-MB-231)	N: 2.5 ± 0.22 (460−470, MDA-MB-231)	40
37	672 (192 600, 5% DMSO in acetonitrile)	—	>80% in 10 min (690, 2.5% DMSO in acetonitrile)	N: 0.91 (SKOV-3)	N: 0.0039 (690, SKOV-3)	233
38	672 (251 000, 5% DMSO in acetonitrile)	—	—	N: 1.28 (SKOV-3)	N: 0.024 (690, SKOV-3)	53
Paclitaxel	—	—	—	—	N: 0.0047 (690, SKOV-3)	—
43	450 (MeOH)	47 (EtOH)	—	N: >200 (MCF-7)	N: 32 ± 3 (450, MCF-7)	6.2
Cisplatin	—	—	—	N: >200 (MCF-7)	>200 (450, MCF-7)	—
44	360 (DMSO)	—	63 (420, DMSO)	>100 (A549)	H: 2.10 ± 0.11; N: 1.23 ± 0.08 (420, A549)	H: 48; N: 83

The fourth factor of comparison is the change in cytotoxicity under normoxia and hypoxia. Comparing IC_{50} and EC_{50} under these conditions, we observe that the change in PI values does not have a unified pattern as well. For example, **1** has a lower PI value under normoxic conditions (H: 1.2 *vs.* N: 0.93), while in the case of **2**, it is higher compared to hypoxia (H: 2.4 *vs.* N: 2.6). In some cases, these values can be found equal. As an example, complex **7** is a ROS-generating compound, for which the PI values are the same under hypoxic and normoxic conditions (H: 7 *vs.* N: 7). Based on this comparison, it can be concluded that there is no clear trend in favor of PI in studies that varied oxygen concentration using the dual PDT/PACT agents.

The fifth comparison factor is the effectiveness of PSs of different natures. Comparing PI values, the gold complex **44** shows higher PI values than ruthenium complexes **1–18** despite their more extensive study (*e.g.*, 83 *vs.* from 1 to 44). Phthalocyanines **35–38** (from 53 to 233) and BODIPYs **30–34** (*e.g.*, 40) also show significant PI value, whereas the binuclear complex **28** (from 3.5 to 25.2) was found to be closer to the ruthenium complexes (from 1 to 44). Consideration of the difference in PI values may also suggest a more favored photoreleasing system.

An important issue is the potential for synergy in this approach to reduce drug dosage and side effects.[16] It could be achieved in the case that the PS remains active after photorelease. By definition, synergy is an interaction of agents or conditions in which the total effect is greater than the sum of the individual effects. According to this definition, an experiment using (1) the PS alone, (2) only a chemotherapeutic agent, (3) both agents together, and (4) neither agent (*i.e.*, control) should be conducted.[105] Such evidence could be obtained, for example, for compound **28** when comparing its efficacy with that of the iridium complex alone, the ruthenium complex, and both of them together. Proof of synergism with this therapy remains an important question in the field.

Most of the presented studies partially lack information that may be important for comparative analysis. To facilitate research in the dual PDT/PACT area, we provide a summary of the methods used for their characterization.

(1) Collection of general photophysical data: measurements of absorption spectra in extinction coefficients and emission spectra, the quantum yield of luminescence,[106–109] the quantum yield of singlet oxygen, and ROS formation using different methods.[63,95,98,110,111]

(2) Photorelease evaluation: measurements of the quantum yield of drug release indicating the wavelength, applied power, time and temperature using actinometry,[16,34,40,90,100] HPLC[35] or LC-MS[98] in the suitable solvent varying the concentration of oxygen; identification of photodegradation products;[11,35,63,72,73,90,98] estimation of the half-life value[112] and the efficacy of the system as the $\varepsilon \cdot \Phi$ value.[66]

(3) Preliminary biological studies: evaluation of stability in the dark at the temperature of biological studies in the solvent in which the photorelease was assessed and then in the buffer and medium that will be used to treat cells;[63] photorelease evaluation indicating the wavelength, applied power, time and temperature varying the concentration of oxygen in the buffer and medium that will be used to treat cells.[35]

(4) *In vitro* biological studies: evaluation of toxicity on multiple cell lines under hypoxia and normoxia varying steeply the concentration of oxygen in the dark and under irradiation[11,16,34–36,63,90,98] and the investigation of localization.[11] If the PS itself is a stable molecule, then it is better to characterize its toxicity and the products of its degradation including the drug. The comparison between PS and PDT/PACT agents can highlight the synergy. For the sake of comparison, IC_{50},[16,63] EC_{50},[74] CC_{50},[11,73] or viability[90] can be estimated depending on the experiment.

(5) Additional sophisticated methods: the bystander effect to investigate the non-irradiated cells located on the edges of the plates such as cells affected only by released drugs due to the diffusion;[83] the Chou–Talalay combination index heat map to understand if the compound can synergize;[34,113] the formation of supramolecular structures and excimers with a consequent concentration increase;[90] the usage of human spheroids to investigate the toxicity towards the hypoxic tumor environment[36,95] or other biological models.[98]

5. Conclusions

Cancer remains one of the leading causes of death worldwide. Therefore, it is necessary to develop effective anticancer therapies. One of such therapies is PDT. PDT has a high spatial and temporal resolution but its use in hypoxia has limitations. These limitations can be overcome by combining this therapy with PACT. By merging these therapies, it is possible to obtain dual PDT/PACT agents based on metal complexes or organic photosynthesizers that effectively kill cancer cells under hypoxia.

Within the framework of this perspective, we have tried to rationalize the properties of compounds possessing great structural variety and that have been tested on very different biological systems. In a comparative analysis, it is found that the more abundant ruthenium complexes on average showed lower PI values compared to, for example, phthalocyanines. When comparing platinum complexes, it is found that varying the nature of the photocage can play a crucial role in the release efficiency, as the nature of the drug itself can affect the release abilities, as shown for BODIPYs. Dual PACT/PDT agents appear as very promising therapeutic agents because of their versatility, but they are also very challenging compounds to design. One of the main challenges is indeed the structural optimization of PS-drug pairing, which requires photophysical and biological studies to find the best combination.

Two additional shortcomings that need to be addressed in the future, independently or simultaneously, should also be underlined. Metal-based PSs are mostly composed of rare and expensive elements and the absence of complexes of more Earth-abundant d-metals can be noted. Low tissue permeability is another problem that, in some cases, authors have tried to overcome by two-photon irradiation or by shifting the absorption spectra to the IR range, but it remains significant in this field.

Overall, we hope that this perspective will help to engage researchers in obtaining new anticancer agents at the interface

of the two therapies, as well as systematize methods for studying such complex systems.

Data availability

No primary research results, software or code have been included and no new data were generated or analysed as part of this review.

Author contributions

K. M. K. wrote the first draft of the manuscript. K. C. and G. G. revised and supervised the manuscript.

Conflicts of interest

The authors declare no conflict of interest.

Acknowledgements

This work was financially supported by an ERC Consolidator Grant PhotoMedMet to G. G. (GA 681679) and by the ANR (COSETTE project) and has received support under the program Investissements d'Avenir launched by the French Government and implemented by the ANR with the reference ANR-10-IDEX-0001-02 PSL (G. G.).

References

1 https://gco.iarc.fr/tomorrow/en/dataviz/isotype.
2 J. R. Lakowicz, in *Principles of fluorescence spectroscopy*, Springer, New York, NY, 3rd edn, 2010, p. 15.
3 L. Gourdon, K. Cariou and G. Gasser, *Chem. Soc. Rev.*, 2022, **51**, 1167–1195.
4 A. Gilbert, J. E. Baggott and P. J. Wagner, in *Essentials of molecular photochemistry*, Blackwell Scientific Publications, London, 1991, pp. 168–170.
5 N. Mehraban and H. Freeman, *Materials*, 2015, **8**, 4421–4456.
6 L. Conti, E. Macedi, C. Giorgi, B. Valtancoli and V. Fusi, *Coord. Chem. Rev.*, 2022, **469**, 214656.
7 P. Fonda-Pascual, O. M. Moreno-Arrones, A. Alegre-Sanchez, D. Saceda-Corralo, D. Buendia-Castaño, C. Pindado-Ortega, P. Fernandez-Gonzalez, K. Velazquez-Kennedy, M. I. Calvo-Sánchez, A. Harto-Castaño, B. Perez-Garcia, L. Bagazgoitia, S. Vaño-Galvan, J. Espada and P. Jaen-Olasolo, *Methods*, 2016, **109**, 190–202.
8 N. J. Farrer, L. Salassa and P. J. Sadler, *Dalton Trans.*, 2009, **28**, 10690–10701.
9 I. M. Dixon, S. Bonnet, F. Alary and J. Cuny, *J. Phys. Chem. Lett.*, 2021, **12**, 7278–7284.
10 G. Bergamini, F. Puntoriero, V. Balzani and S. Campagna, in *Topics in Current Chemistry*, Springer, Berlin, Heidelberg, 2007, vol. 280, pp. 1–36.
11 C. Zhang, R. Guan, X. Liao, C. Ouyang, T. W. Rees, J. Liu, Y. Chen, L. Ji and H. Chao, *Chem. Commun.*, 2019, **55**, 12547–12550.
12 V. H. S. Van Rixel, V. Ramu, A. B. Auyeung, N. Beztsinna, D. Y. Leger, L. N. Lameijer, S. T. Hilt, S. E. Le Dévédec, T. Yildiz, T. Betancourt, M. B. Gildner, T. W. Hudnall, V. Sol, B. Liagre, A. Kornienko and S. Bonnet, *J. Am. Chem. Soc.*, 2019, **141**, 18444–18454.
13 A. Busemann, I. Flaspohler, X.-Q. Zhou, C. Schmidt, S. K. Goetzfried, V. H. S. Van Rixel, I. Ott, M. A. Siegler and S. Bonnet, *J. Biol. Inorg. Chem.*, 2021, **26**, 667–674.
14 Q. Chen, J.-A. Cuello-Garibo, L. Bretin, L. Zhang, V. Ramu, Y. Aydar, Y. Batsiun, S. Bronkhorst, Y. Husiev, N. Beztsinna, L. Chen, X.-Q. Zhou, C. Schmidt, I. Ott, M. J. Jager, A. M. Brouwer, B. E. Snaar-Jagalska and S. Bonnet, *Chem. Sci.*, 2022, **13**, 6899–6919.
15 B. A. Albani, B. Peña, N. A. Leed, N. A. B. G. De Paula, C. Pavani, M. S. Baptista, K. R. Dunbar and C. Turro, *J. Am. Chem. Soc.*, 2014, **136**, 17095–17101.
16 L. N. Lameijer, D. Ernst, S. L. Hopkins, M. S. Meijer, S. H. C. Askes, S. E. Le Dévédec and S. Bonnet, *Angew. Chem., Int. Ed.*, 2017, **56**, 11549–11553.
17 D. M. Gilkes, G. L. Semenza and D. Wirtz, *Nat. Rev. Cancer*, 2014, **14**, 430–439.
18 S. A. McFarland, A. Mandel, R. Dumoulin-White and G. Gasser, *Curr. Opin. Chem. Biol.*, 2020, **56**, 23–27.
19 A. Gandosio, K. Purkait and G. Gasser, *Chimia*, 2021, **75**, 845.
20 M. Wysocki, B. Czarczynska-Goslinska, D. Ziental, M. Michalak, E. Güzel and L. Sobotta, *ChemMedChem*, 2022, **17**, e202200185.
21 M. Overchuk, R. A. Weersink, B. C. Wilson and G. Zheng, *ACS Nano*, 2023, **17**, 7979–8003.
22 Y. Zhao, X. Liu, X. Liu, J. Yu, X. Bai, X. Wu, X. Guo, Z. Liu and X. Liu, *Front. Immunol.*, 2022, **13**, 955920.
23 A. Bienia, O. Wiecheć-Cudak, A. A. Murzyn and M. Krzykawska-Serda, *Pharmaceutics*, 2021, **13**, 1147.
24 D. Viswanath and Y.-Y. Won, *Biomater. Sci.*, 2022, **8**, 3644–3658.
25 L. Menilli, C. Milani, E. Reddi and F. Moret, *Cancers*, 2022, **14**, 4462.
26 E. C. Glazer, *Isr. J. Chem.*, 2013, **53**, 391–400.
27 Y.-L. Yang, K. Lin and L. Yang, *Pharmaceutics*, 2021, **13**, 1951.
28 R. Weinstain, T. Slanina, D. Kand and P. Klán, *Chem. Rev.*, 2020, **120**, 13135–13272.
29 S. Bonnet, *J. Am. Chem. Soc.*, 2023, **145**, 23397–23415.
30 P. C. Ford, D. Wink and J. Dibenedetto, in *Progress in Inorganic Chemistry*, ed. S. J. Lippard, Wiley, 1st edn, 1983, vol. 30, pp. 213–271.
31 C. Wegeberg and O. S. Wenger, *JACS Au*, 2021, **1**, 1860–1876.
32 Y. Chen, L. Bai, P. Zhang, H. Zhao and Q. Zhou, *Molecules*, 2021, **26**, 5679.
33 A. Zamora, C. A. Denning, D. K. Heidary, E. Wachter, L. A. Nease, J. Ruiz and E. C. Glazer, *Dalton Trans.*, 2017, **46**, 2165–2173.
34 N. Toupin, S. J. Steinke, S. Nadella, A. Li, T. N. Rohrabaugh, E. R. Samuels, C. Turro, I. F. Sevrioukova and J. J. Kodanko, *J. Am. Chem. Soc.*, 2021, **143**, 9191–9205.

35 D. Havrylyuk, A. C. Hachey, A. Fenton, D. K. Heidary and E. C. Glazer, *Nat. Commun.*, 2022, **13**, 3636.
36 C. Zhang, X. Guo, X. Da, Z. Wang, X. Wang and Q. Zhou, *Dalton Trans.*, 2021, **50**, 10845–10852.
37 L. N. Lameijer, C. Van De Griend, S. L. Hopkins, A.-G. Volbeda, S. H. C. Askes, M. A. Siegler and S. Bonnet, *J. Am. Chem. Soc.*, 2019, **141**, 352–362.
38 J. Cuello-Garibo, C. C. James, M. A. Siegler, S. L. Hopkins and S. Bonnet, *Chem.–Eur. J.*, 2019, **25**, 1260–1268.
39 V. H. S. Van Rixel, B. Siewert, S. L. Hopkins, S. H. C. Askes, A. Busemann, M. A. Siegler and S. Bonnet, *Chem. Sci.*, 2016, **7**, 4922–4929.
40 J. D. Knoll, B. A. Albani and C. Turro, *Chem. Commun.*, 2015, **51**, 8777–8780.
41 L. M. Loftus, J. J. Rack and C. Turro, *Chem. Commun.*, 2020, **56**, 4070–4073.
42 J. D. Knoll, B. A. Albani and C. Turro, *Acc. Chem. Res.*, 2015, **48**, 2280–2287.
43 A. J. Göttle, F. Alary, M. Boggio-Pasqua, I. M. Dixon, J.-L. Heully, A. Bahreman, S. H. C. Askes and S. Bonnet, *Inorg. Chem.*, 2016, **55**, 4448–4456.
44 K. Eastham, P. A. Scattergood, D. Chu, R. Z. Boota, A. Soupart, F. Alary, I. M. Dixon, C. R. Rice, S. J. O. Hardman and P. I. P. Elliott, *Inorg. Chem.*, 2022, **61**, 19907–19924.
45 J. D. Knoll, B. A. Albani, C. B. Durr and C. Turro, *J. Phys. Chem. A*, 2014, **118**, 10603–10610.
46 S. E. Greenough, G. M. Roberts, N. A. Smith, M. D. Horbury, R. G. McKinlay, J. M. Żurek, M. J. Paterson, P. J. Sadler and V. G. Stavros, *Phys. Chem. Chem. Phys.*, 2014, **16**, 19141–19155.
47 B. A. Albani, C. B. Durr and C. Turro, *J. Phys. Chem. A*, 2013, **117**, 13885–13892.
48 T. N. Rohrabaugh, A. M. Rohrabaugh, J. J. Kodanko, J. K. White and C. Turro, *Chem. Commun.*, 2018, **54**, 5193–5196.
49 R. Wang, T. A. Eberspacher, T. Hasegawa, V. Day, D. C. Ware and H. Taube, *Inorg. Chem.*, 2001, **40**, 593–600.
50 C. Imberti, P. Zhang, H. Huang and P. J. Sadler, *Angew. Chem., Int. Ed. Engl.*, 2020, **59**, 61–73.
51 U. Schatzschneider, *Eur. J. Inorg. Chem.*, 2010, **2010**, 1451–1467.
52 A. Mani, T. Feng, A. Gandioso, R. Vinck, A. Notaro, L. Gourdon, P. Burckel, B. Saubaméa, O. Blacque, K. Cariou, J. Belgaied, H. Chao and G. Gasser, *Angew. Chem., Int. Ed.*, 2023, **62**, e202218347.
53 M. Huynh, R. Vinck, B. Gibert and G. Gasser, *Adv. Mater.*, 2024, **36**, 2311437.
54 X. Xue, Y. Fu, L. He, L. Salassa, L.-F. He, Y.-Y. Hao, M. J. Koh, C. Soulié, R. J. Needham, A. Habtemariam, C. Garino, K. A. Lomachenko, Z. Su, Y. Qian, M. J. Paterson, Z.-W. Mao, H.-K. Liu and P. J. Sadler, *Inorg. Chem.*, 2021, **60**, 17450–17461.
55 H. Huang, S. Banerjee and P. J. Sadler, *ChemBioChem*, 2018, **19**, 1574–1589.
56 R. Das, U. Das, N. Roy, C. Mukherjee, S. U and P. Paira, *Dyes Pigm.*, 2024, **226**, 112134.
57 N. Wu, J.-J. Cao, X.-W. Wu, C.-P. Tan, L.-N. Ji and Z.-W. Mao, *Dalton Trans.*, 2017, **46**, 13482–13491.
58 S. Kolemen, T. Ozdemir, D. Lee, G. M. Kim, T. Karatas, J. Yoon and E. U. Akkaya, *Angew. Chem., Int. Ed.*, 2016, **55**, 3606–3610.
59 L. A. Hu, Y. Zhang, Q. Zhang, Q. Yin and X. Zhang, *Angew. Chem., Int. Ed.*, 2020, **59**, 5321–5325.
60 J. Zeng, X. Wang, Y. Qi, Y. Yu, X. Zeng and X. Zhang, *Angew. Chem., Int. Ed.*, 2019, **58**, 5692–5696.
61 S. Kuang, L. Sun, X. Zhang, X. Liao, T. W. Rees, L. Zeng, Y. Chen, X. Zhang, L. Ji and H. Chao, *Angew. Chem., Int. Ed.*, 2020, **59**, 20697–20703.
62 S. Kuang, F. Wei, J. Karges, L. Ke, K. Xiong, X. Liao, G. Gasser, L. Ji and H. Chao, *J. Am. Chem. Soc.*, 2022, **144**, 4091–4101.
63 Y. Peng, X. Da, W. Zhou, Y. Xu, X. Liu, X. Wang and Q. Zhou, *Dalton Trans.*, 2024, **53**, 3579–3588.
64 H. Li, C. Xie, R. Lan, S. Zha, C.-F. Chan, W.-Y. Wong, K.-L. Ho, B. D. Chan, Y. Luo, J.-X. Zhang, G.-L. Law, W. C. S. Tai, J.-C. G. Bünzli and K.-L. Wong, *J. Med. Chem.*, 2017, **60**, 8923–8932.
65 A. Loudet and K. Burgess, *Chem. Rev.*, 2007, **107**, 4891–4932.
66 P. Shrestha, D. Kand, R. Weinstain and A. H. Winter, *J. Am. Chem. Soc.*, 2023, **145**, 17497–17514.
67 P.-C. Lo, M. S. Rodríguez-Morgade, R. K. Pandey, D. K. P. Ng, T. Torres and F. Dumoulin, *Chem. Soc. Rev.*, 2020, **49**, 1041–1056.
68 C. M. Allen, W. M. Sharman and J. E. Van Lier, *J. Porphyrins Phthalocyanines*, 2001, **05**, 161–169.
69 N. Rubinstein, P. Liu, E. W. Miller and R. Weinstain, *Chem. Commun.*, 2015, **51**, 6369–6372.
70 P. Shrestha, A. Mukhopadhyay, K. C. Dissanayake and A. H. Winter, *J. Org. Chem.*, 2022, **87**, 14334–14341.
71 P. P. Goswami, A. Syed, C. L. Beck, T. R. Albright, K. M. Mahoney, R. Unash, E. A. Smith and A. H. Winter, *J. Am. Chem. Soc.*, 2015, **137**, 3783–3786.
72 M. Liu, J. Meng, W. Bao, S. Liu, W. Wei, G. Ma and Z. Tian, *ACS Appl. Bio Mater.*, 2019, **2**, 3068–3076.
73 E. M. Digby, S. Ayan, P. Shrestha, E. J. Gehrmann, A. H. Winter and A. A. Beharry, *J. Med. Chem.*, 2022, **65**, 16679–16694.
74 N. P. Toupin, K. Arora, P. Shrestha, J. A. Peterson, L. J. Fischer, E. Rajagurubandara, I. Podgorski, A. H. Winter and J. J. Kodanko, *ACS Chem. Biol.*, 2019, **14**, 2833–2840.
75 **https://www.accessdata.fda.gov/drugsatfda_docs/label/2011/010669s032lbl.pdf**.
76 D. Steverding, *Open Enzyme Inhib. J.*, 2011, **4**, 11–16.
77 O. Lockridge, D. M. Quinn and Z. Radić, in *Comprehensive Toxicology*, Elsevier, 2018, vol. 10, pp. 277–307.
78 K. Honey, T. Nakagawa, C. Peters and A. Rudensky, *J. Exp. Med.*, 2002, **195**, 1349–1358.
79 W. Fitch, E. T. MacKenzie and A. M. Harper, *Circ. Res.*, 1975, **37**, 550–557.
80 K. Sitkowska, B. L. Feringa and W. Szymański, *J. Org. Chem.*, 2018, **83**, 1819–1827.

81 M. D. Maree, N. Kuznetsova and T. Nyokong, *J. Photochem. Photobiol., A*, 2001, **140**, 117–125.
82 M. Bio, G. Nkepang and Y. You, *Chem. Commun.*, 2012, **48**, 6517.
83 A. M. L. Hossion, M. Bio, G. Nkepang, S. G. Awuah and Y. You, *ACS Med. Chem. Lett.*, 2013, **4**, 124–127.
84 M. Bio, P. Rajaputra, G. Nkepang and Y. You, *J. Med. Chem.*, 2014, **57**, 3401–3409.
85 P. Thapa, M. Li, M. Bio, P. Rajaputra, G. Nkepang, Y. Sun, S. Woo and Y. You, *J. Med. Chem.*, 2016, **59**, 3204–3214.
86 **https://www.accessdata.fda.gov/scripts/opdlisting/oopd/detailedIndex.cfm?cfgridkey=167503**.
87 **https://www.accessdata.fda.gov/drugsatfda_docs/nda/2002/75278_Paclitaxel.cfm**.
88 X.-J. Jiang, S.-L. Yeung, P.-C. Lo, W.-P. Fong and D. K. P. Ng, *J. Med. Chem.*, 2011, **54**, 320–330.
89 X.-J. Jiang, P.-C. Lo, S.-L. Yeung, W.-P. Fong and D. K. P. Ng, *Chem. Commun.*, 2010, **46**, 3188.
90 E. D. Anderson, A. P. Gorka and M. J. Schnermann, *Nat. Commun.*, 2016, **7**, 13378.
91 S. Xu, X. Zhu, C. Zhang, W. Huang, Y. Zhou and D. Yan, *Nat. Commun.*, 2018, **9**, 2053.
92 **https://precision.fda.gov/uniisearch/srs/unii/5S2CCF3T1Z**.
93 P. S. Chelushkin, J. R. Shakirova, I. S. Kritchenkov, V. A. Baigildin and S. P. Tunik, *Dalton Trans.*, 2022, **51**, 1257–1280.
94 D. Jaque, L. Martínez Maestro, B. Del Rosal, P. Haro-Gonzalez, A. Benayas, J. L. Plaza, E. Martín Rodríguez and J. García Solé, *Nanoscale*, 2014, **6**, 9494–9530.
95 O. O. Krasnovskaya, R. A. Akasov, D. V. Spector, K. G. Pavlov, A. A. Bubley, V. A. Kuzmin, A. A. Kostyukov, E. V. Khaydukov, E. V. Lopatukhina, A. S. Semkina, K. Yu. Vlasova, S. A. Sypalov, A. S. Erofeev, P. V. Gorelkin, A. N. Vaneev, V. N. Nikitina, D. A. Skvortsov, D. A. Ipatova, D. M. Mazur, N. V. Zyk, D. A. Sakharov, A. G. Majouga and E. K. Beloglazkina, *ACS Appl. Mater. Interfaces*, 2023, **15**, 12882–12894.
96 **https://www.accessdata.fda.gov/drugsatfda_docs/label/2011/018057s080lbl.pdf**.
97 **https://precision.fda.gov/uniisearch/srs/unii/Q20Q21Q62J**.
98 Y. Luo, B. Cao, M. Zhong, M. Liu, X. Xiong and T. Zou, *Angew. Chem., Int. Ed. Engl.*, 2022, **61**, e202212689.
99 T. Shao and Y.-L. Chen, *J. Hepatol.*, 2024, **80**, e200–e201.
100 A. Bahreman, J.-A. Cuello-Garibo and S. Bonnet, *Dalton Trans.*, 2014, **43**, 4494–4505.
101 Y. Wang, L. Xie and J. Ni, in *Cytochrome P450*, ed. Z. Yan and G. W. Caldwell, Springer US, New York, NY, 2021, pp. 121–139.
102 A. A. Stratonnikov, A. Y. Douplik, D. V. Klimov, V. B. Loschenov and S. V. Mizin, *Optical Methods for Tumor Treatment and Detections: Mechanisms and Techniques in Photodynamic Therapy VII*, ed. T. J. Dougherty, San Jose, CA, 1998, vol. 3247, pp. 128–136.
103 N. Bustamante, G. Ielasi, M. Bedoya and G. Orellana, *Polymers*, 2018, **10**, 234.
104 M. Dramićanin, in *Luminescence thermometry: methods, materials, and applications*, Woodhea Publishing, Duxford, United Kingdom, 2018, pp. 31–62.
105 B. K. Slinker, *J. Mol. Cell. Cardiol.*, 1998, **30**, 723–731.
106 **https://static.horiba.com/fileadmin/Horiba/Application/Materials/Material_Research/Quantum_Dots/quantumyieldstrad.pdf**.
107 A. T. R. Williams, S. A. Winfield and J. N. Miller, *Analyst*, 1983, **108**, 1067.
108 C. Würth, C. Lochmann, M. Spieles, J. Pauli, K. Hoffmann, T. Schüttrigkeit, T. Franzl and U. Resch-Genger, *Appl. Spectrosc.*, 2010, **64**, 733–741.
109 A. M. Brouwer, *Pure Appl. Chem.*, 2011, **83**, 2213–2228.
110 J. F. Woolley, J. Stanicka and T. G. Cotter, *Trends Biochem. Sci.*, 2013, **38**, 556–565.
111 K. Yan, A. C. Sedgwick, Y. Zang, G. Chen, X. He, J. Li, J. Yoon and T. D. James, *Small Methods*, 2019, **3**, 1900013.
112 K. Sitkowska, M. F. Hoes, M. M. Lerch, L. N. Lameijer, P. Van Der Meer, W. Szymański and B. L. Feringa, *Chem. Commun.*, 2020, **56**, 5480–5483.
113 T.-C. Chou, *Cancer Res.*, 2010, **70**, 440–446.